



Canadian Journal of Earth Sciences

Petrography, geochemistry and Nd isotope systematics of metaconglomerates and matrix-rich metasedimentary rocks: Implications for the provenance and tectonic setting of the Labrador Trough, Canada

Journal:	<i>Canadian Journal of Earth Sciences</i>
Manuscript ID	cjes-2018-0187.R2
Manuscript Type:	Article
Date Submitted by the Author:	11-Nov-2018
Complete List of Authors:	Henrique-Pinto, Renato; Universite Laval Faculte des sciences et de genie, Département de géologie et de génie géologique Guilmette, Carl; Universite Laval Faculte des sciences et de genie Bilodeau, Carl; Ministere de l'Energie et des Ressources naturelles Stevenson, Ross; GEOTOP Carvalho, Bruna; Università degli Studi di Padova; Dipartimento di Geoscienze, via G. Gradenigo, 6 - 35131 Padova, Italy.
Keyword:	Provenance; Nd systematics; granitic clasts; juvenile sources; metasedimentary geochemistry.
Is the invited manuscript for consideration in a Special Issue? :	Not applicable (regular submission)

SCHOLARONE™
Manuscripts

1 **Title: Petrography, geochemistry and Nd isotope systematics of metaconglomerates**
2 **and matrix-rich metasedimentary rocks: Implications for the provenance and**
3 **tectonic setting of the Labrador Trough, Canada**

4

5 **Authors:** Henrique-Pinto, R.¹; Guilmette, C.¹; Bilodeau, C.²; Stevenson, R.³; Carvalho, B.B.⁴

6

7 **Affiliations:**

8 ¹ Université Laval; e4M, Département de géologie et de génie géologique, 1065 Avenue de la
9 Médecine, Québec, QC G1V 0A6.

10 ² Ministère de l'Énergie et Ressources Naturelles du Québec; 5700, 4e Avenue Ouest, Québec,
11 A301.

12 ³ GEOTOP; Département des Sciences de la Terre et de l'Atmosphère, Université du Québec à
13 Montréal, Montréal, QC H2X 3Y7, Canada.

14 ⁴ Università degli Studi di Padova; Dipartimento di Geoscienze, via G. Gradenigo, 6 - 35131
15 Padova, Italy.

16

17

18 **Corresponding author:** renato.henrique-pinto.1@ulaval.ca

19

1 Abstract

2 The New Quebec Orogen consists of a supracrustal belt that was reworked when the Superior craton
3 collided with the Core Zone terrane during the Paleoproterozoic Trans-Hudson Orogeny. Within the New
4 Quebec Orogen, the Kaniapiskau Supergroup can be divided into four terrigenous lithotypes metamorphosed
5 at low-grade: one set with greater compositional and textural sedimentary maturity classified as quartz
6 arenites and subarkoses, and another set with lower textural maturity classified as feldspathic wackes and
7 mudrocks. In contrast, the Laporte Group includes homogeneous lithotypes represented by feldspathic and
8 lithic wackes with a range of matrix contents metamorphosed at low to medium-grade.

9 The Kaniapiskau Supergroup rocks have a wide range of SiO_2 and Al_2O_3 contents ($\text{SiO}_2/\text{Al}_2\text{O}_3 =$
10 3.7-51) compared to the restricted compositional range of the Laporte Group rocks ($\text{SiO}_2/\text{Al}_2\text{O}_3 = 4.4-6.8$).
11 In general, the geochemical variations in both formations of the Laporte Group are within the range of the
12 main clast varieties from basal metaconglomerates, although the Deborah Formation (top unit), records
13 higher TiO_2 , P_2O_5 , MgO and Ni contents and high Cr/Th , Co/Ba , Th/U and Rb/Sr ratios indicating additional
14 mafic sources.

15 Our results support the hypothesis that the Kaniapiskau Supergroup was deposited along an
16 intraplate continental margin with predominantly recycled ($\epsilon\text{Nd}_{(1.87\text{Ga})} -12$) Paleoproterozoic sources (TDM 3.2
17 Ga). In contrast, the Laporte Group marks the transition from a continental forearc (Grand Rosoy Fm.) with
18 a typical juvenile source, including granitic clasts ($\epsilon\text{Nd}_{(1.83\text{Ga})} -0.1$ to $+3.1$), to a wedge-top depozone (Deborah
19 Fm.) in the context of a collisional pro-foreland basin. This syn-collisional sedimentary environment is
20 characterized by the presence of old crustal components ($\epsilon\text{Nd}_{(1.83\text{Ga})} -4.4$ to -9.1).

21
22 **Keywords:** Provenance; Nd systematics; granitic clasts; juvenile sources; metasedimentary geochemistry.

25 1. Introduction

26 Sedimentary rocks with high textural maturity do not typically preserve mafic and
27 intermediate sources as lithic fragments or as components in the main population of detrital zircons.
28 Mafic to intermediate sources are usually easily weathered and deposited as fine-grained sediments
29 (e.g., Nesbitt and Young, 1982; Nesbitt et al., 1996; Nesbitt and Young, 1996). Thus, the
30 contribution of the mafic sources to a sedimentary basin requires an investigation of matrix-rich
31 conglomerates, wackes and mudrocks.

1 The study of clasts in polymictic conglomerates provides a direct window to understand
2 the principal sources for the basin (e.g., Naqvi et al., 1878; Reimer et al., 1985; Biševac et al., 2011;
3 Henrique-Pinto et al., 2012). Likewise, matrix-rich sedimentary rocks require a combination of
4 provenance tools to evaluate stratigraphic and tectonic settings (e.g., Bhatia, 1985; Cox et al., 1995;
5 McLennan et al., 1995; Henrique-Pinto et al., 2015).

6 Provenance studies provide key information about paleogeography, which may be
7 challenging in cases where even well-studied geological sequences have ambiguous
8 tectonic/stratigraphic interpretations (e.g., New Quebec Orogen in western Canada; Henrique-Pinto
9 et al., 2017). This ambiguity can be resolved using combined complementary provenance tools,
10 such as petrography, geochemistry, and Nd isotope systematics that have proven to be important
11 instruments in determining the relative contributions of felsic and mafic sources, as well as the
12 tectonic setting and crustal evolution trends for metasedimentary rocks (e.g., McLennan et al.,
13 1990; McLennan and Hemming, 1991; McLennan et al., 1993).

14 The New Quebec Orogen (Hoffman, 1988; Hoffman, 1990a) is an exceptional example of
15 one of the most ancient Wilson cycle sedimentary records from the Manikewan paleo-ocean
16 (Stauffer, 1984). The closure and amalgamation of the continental blocks that once separated the
17 Superior from the surrounding North Atlantic, Rae and Hearne cratons, marks the final phase of
18 the Trans-Hudson Orogen (1.83-1.80 Ga) and the consolidation of a large continental block of
19 Laurentia (Hoffman, 1989a; Hoffman, 1989b and Hoffman, 1990b) with the blocks of Siberia and
20 Baltica (Meert, 2012) to form the Nuna super landmass (Hoffman, 1997), the largest core element
21 of the Columbia Supercontinent (e.g., Rogers and Santosh, 2002; Zhao et al., 2004).

22 Within the New Quebec Orogen, the Labrador Trough consists of greenschist facies
23 sedimentary and volcanic sequences (Kaniapiskau Supergroup; Frarey and Duffell, 1964), inferred
24 to represent the rifted margin of the Superior Craton and a potential oceanic domain (e.g., Atlantic-
25 type passive margin; Boone and Hynes, 1990). Further east, the Laporte Group (Fahrig, 1952;

1 Harrison, 1952) is composed of similar successions of unclear origin that were metamorphosed to
2 higher grades.

3 The Kaniapiskau Supergroup includes two main volcano-sedimentary cycles (2.17-2.14
4 Ga and 1.88-1.87 Ga) and a third cycle that unconformably overlies the earlier strata (e.g., Clark,
5 1988). It generally accepted that the first cycle of sedimentation accumulated in an intracontinental
6 rift-related environment (Clark and Wares, 2005, and references therein). The tectonic environment
7 of the transition to subsequent cycles is debated and has been suggested to be represented by the
8 transition from a rifted margin to a foreland basin (e.g., Hoffman, 1987, 1988, 1990a), or the
9 transition from a rift to a passive margin in a shallow platformal ocean basin that was synchronous
10 with upper plate continental forearc sedimentation in an Andean-type magmatic arc context (Van
11 der Leeden et al., 1990).

12 In light of these contradictory tectonic interpretations, this contribution reports, for the first
13 time, Sm-Nd isotopic data combined with geochemical and petrographic analyses of polymictic
14 clasts from metaconglomerates and matrix-rich metasedimentary rocks of the Labrador Trough that
15 shed light on the nature and evolution of different basins within the New Quebec Orogen.

16 **2. Geological setting**

17 **2.1. Labrador Trough**

18 The Labrador Trough is a NW-SE elongated supracrustal fold belt that extends more than
19 850 km from Ungava Bay, in the north, to the Grenville Province, in the south (Clark and Wares,
20 2005), separating the Superior Craton from the Core Zone (James et al., 1996). The Core Zone is
21 considered an Archean to Paleoproterozoic microcontinent (Wardle et al., 2002; Corrigan et al.,
22 2009) that collided in the east with the Nain Province block (North Atlantic Craton) at ca. 1.87-
23 1.85 Ga to form the Torngat Orogen, and in the west with the Superior Craton ca. 1.82-1.77 Ga to
24 form the New Quebec Orogen (Hoffman, 1988; Hoffman, 1990a) (Fig.1).

1 Both the New Quebec and Torngat orogens are considered subdivisions of the Trans-
2 Hudson Orogen (Corrigan et al., 2009; Eaton and Darbyshire, 2010) that formed during the closure
3 of the Manikewan Ocean (Stauffer, 1984). This ocean basin separated the Superior from the
4 surrounding North Atlantic, Rae and Hearne cratons (collectively referred to as the Churchill
5 Province; Hoffman, 1988; Lewry and Collerson, 1990).

6 The New Quebec Orogen (e.g., Hoffman, 1988; Wardle et al., 2002; Clark and Wares,
7 2005) is subdivided into four main lithotectonic domains: (1) the western autochthonous domain
8 consisting of low-grade metavolcanic and metasedimentary rocks (Kaniapiskau Supergroup: Frarey
9 and Duffell, 1964); (2) a central metavolcano-sedimentary belt with voluminous gabbro sills and
10 pillow-lava basalts; (3) the east-central (allochthonous?) Rachel-Laporte Zone, consisting of
11 medium- to high-grade supracrustal rocks (Laporte Group: Fahrig, 1952; Harrison, 1952) and
12 gneissic-migmatitic Archean basement of poorly constrained origins (e.g., Boulder, Rénia and
13 Moyer gneiss complexes: Gélinas, 1965), which, according to some authors, represent windows
14 and tectonic slices of the Superior basement (James et al., 1996; James and Dunning, 2000; Simard
15 et al., 2013); and (4) the eastern amphibolite facies schists and gneisses that border the Kuujjuaq
16 Domain (Manereuille Complex? Girard, 1995) and possibly belonging to the Core Zone (e.g.,
17 Akiasirviup, Curot and False suites; Charette et al., 2016) (Fig. 2).

18

19 **2.1.1. Kaniapiskau Supergroup**

20 The beginning of the first cycle of sedimentation within the Kaniapiskau Supergroup is
21 characterized by the Seward Group (2169 ± 4 Ma; Rohon et al., 1993), which represents an
22 intracratonic rift basin that begins with the deposition of mainly immature arkosic arenites and
23 conglomerates (Baragar, 1967), accompanied by contemporaneous mafic volcanic activity
24 (Chakonipau Formation) (Fig. 3).

1 The Pistolet Group (2.17–2.14 Ga; Melezhik et al., 1997) marks the transition from rift to
2 passive margin platform as suggested by the presence of dolomites, calc-arenites and mudrocks.
3 The Pistolet Group is overlain by black shales, basalts and rhyolite dykes (Bacchus Formation) of
4 the Swampy Bay Group (2142 ± 4 Ma; Rohon et al., 1993).

5 The end of the first cycle of sedimentation is marked by the presence of a dolomitic reef
6 complex (Attikamagen Group). The reef was deposited under storm-influenced evaporitic
7 conditions in the middle and outer portions of the shallow ramp of the Denault Formation
8 (Zentmyer et al., 2011) but has a poorly defined age (see discussion in Henrique-Pinto et al., 2017).

9 The beginning of Ferriman Group sedimentation includes sandstones of the Wishart
10 Formation and mudrocks of the Ruth Formation. These formations are followed by the Sokoman
11 iron formation (e.g., Dimroth and Chauvel, 1973; Klein and Fink, 1976), reflecting a transitional
12 sedimentary environment that consists of lagoonal platform sediments deposited in a warm and dry
13 climate (Chauvel and Dimroth, 1974).

14 The upper Ferriman Group is consists of distal euxinic black shales and turbidites of the
15 Menihék Formation, marking the second cycle of sedimentation of the Kaniapiskau Supergroup.
16 Eastward correlation with the distal sedimentary sequences of the Koksoak Group (1870 ± 4 Ma;
17 Machado et al., 1997) is reported by Clark and Wares (2005). Similarities between the Sokoman
18 Formation and the middle units of the Baby Formation are suggested by lateral stratigraphic
19 correlations and rare earth element profiles (Clark, 1988).

20 The red-bed arkoses and conglomerates from the Chioak and Tamarack River formations,
21 unconformably overlie the earlier sequences and are interpreted as a fluvio-deltaic “synorogenic
22 molasse” (Clark, 1988). These formations lack any volcanic association and mark the third cycle
23 of sedimentation of the Kaniapiskau Supergroup (Clark and Wares, 2005) (Fig. 3).

1

2 **2.1.2. Laporte Group**

3 Girard (1995) divided the Laporte Group into two main formations. The Grand Rosoy
4 Formation forms the base of the group and is dominated by arkosic metasedimentary rocks with
5 local subordinate layers of metaconglomerate containing centimetric hematite clasts. The overlying
6 Deborah Formation is thicker and is composed of phyllite and metawacke with thin layers of
7 amphibolite and graphite schist (black shales).

8 Girard (1995) classified the rocks of the Manereuille Complex as part of the Laporte Group.
9 However, all contacts observed between the complex and the Deborah/Grand Rosoy formations in
10 this study were consistently tectonic. Most rocks from the Manereuille Complex occur near the
11 gneisses of the Kuujjuaq Domain, and whether they belong to the Rachel-Laporte Zone (Wardle et
12 al., 2002) remains a matter of debate.

13 No minimum age of sedimentation, or detrital zircon provenance, has been reported for the
14 Laporte Group. However, monazite and titanite geochronology of amphibolite-facies gneisses
15 within the Rachel-Laporte Zone yielded ages 1793 ± 5 and 1769 ± 5 Ma (Machado et al., 1989;
16 Machado, 1990). Rutile geochronology was also used to date the youngest and final metamorphic
17 event of Hudsonian metamorphism in the New Quebec Orogen (1740 ± 5 Ma; Machado et al.,
18 1989).

19

20 **3. Analytical procedures**

21 **3.1. Rock samples**

22 The samples used in this study are representative of the Kaniapiskau Supergroup and
23 Laporte Group metasedimentary successions (Fig. 2) in terms of grain size, composition and
24 textural maturity. The samples were collected from the best available exposures to avoid the effects

1 of weathering. Thirty-two samples were selected for whole-rock geochemistry and twelve for Sm-
2 Nd isotope analyses. The chemical analyses were preceded by petrographic studies and modal
3 counting, with more than 700 points counted per thin section (Table 1).

4

5 **3.2. Whole-rock chemistry**

6 Geochemical analyses of 10 samples from Kaniapiskau Supergroup and 22 samples from
7 Laporte Group were carried out at the Actlabs facility of Ontario (Canada) and the results are
8 presented in the Table S1. Samples were first crushed in a steel jaw-crusher and then in an agate
9 disk mill. Whole-rock major elements were analysed by heavy absorber fusion technique (Norrish
10 and Hutton, 1969). Prior to fusion, loss on ignition (LOI) was determined from the weight lost after
11 roasting the sample at 1,000°C.

12 The fusion disk was made by mixing 0.75 g equivalent of the roasted sample with a 9.75 g
13 combination of lithium metaborate and lithium tetraborate, with lithium bromide as a releasing
14 agent. Samples were analysed by Panalytical Axios Advanced wavelength dispersive X-Ray
15 Fluorescence (XRF). The intensities were measured and the concentrations calculated against the
16 standard G16. In general, the limit of detection is about 0.01 wt% for most elements.

17 Trace element compositions were obtained by pressed powder pellet made from 6 g of
18 sample. Samples were measured by Panalytical Axios Advanced wavelength dispersive XRF with
19 limits of detection between 1 and 5 ppm. Elements including Cd, Cu, Ag, Ni, Mo, Zn and S were
20 obtained by total digestion-ICP-MS.

21 Ultra-trace element compositions for Au, As, Br, Cr, Ir, Sc, Sb and Se were obtained by
22 INAA (Instrumental Neutron Activation), following the analytical protocol described in Hoffman
23 (1992). Samples were analysed using a Varian Vista 735 ICP.

24

1 3.3. Sm-Nd analyses

2 Whole-rock Sm-Nd isotope analyses were performed on the same samples used for
3 elemental geochemistry at the Geotop laboratory of Université du Québec à Montréal in Montreal
4 (Canada). A 0.1 ± 0.01 g subsample was weighed and spiked with a $^{150}\text{Nd} - ^{49}\text{Sm}$ tracer solution to
5 determine Sm-Nd concentrations. A mixture of HF-HNO₃ acids was added and the mixture placed
6 in an oven to dissolve the samples at a temperature of 150°C. The resulting salts were subsequently
7 evaporated in perchloric acid to break up the fluoride salts and redissolved in 6 mol/L HCl in the
8 oven for 12 h. The subsequent 6 mol/L HCl solution was loaded onto ion-exchange columns
9 containing AG1X8 resin that retains the Fe in the sample but allowed the other elements to be
10 eluted with 6 mol/L HCl. The samples were evaporated and 0.5 mL of 14 mol/L HNO₃ was added
11 to convert the salts from chlorides to nitrates. The rare-earth elements (REE) were concentrated
12 using Eichrom TRU Spec resin for which samples must be nearly Fe-free. About 1mL of TRU Spec
13 resin was placed in the column washed with 3-4 mL of 0.05 mol/L HNO₃ and equilibrated using 2
14 mL of 1 mol/L HNO₃ prior to loading 1mL of the samples. The column was rinsed with 0.25 mL
15 of 0.05 mol/L HNO₃ and the REE fractions collected using 1.75 mL of 0.05 mol/L HNO₃.

16 The Sm–Nd separation was achieved using columns containing about 2 mL of Eichrom LN
17 Spec resin. These columns were conditioned with 0.2 mol/L HCl prior to loading the samples in
18 the same acid. The light REE were eluted with 0.2 mol/L HCl and then Nd was collected using 0.3
19 mol/L HC and Sm was collected using 0.5 mol/L HCl.

20 The isotopic compositions and concentrations of Nd were analysed by thermal ionization
21 mass spectrometry (TIMS) on a TRITON PLUS mass spectrometer. Nd and Sm were measured
22 using a double Re filament assemblage with the samples loaded and evaporated on one filament
23 and ionized by the second filament. The Sm and Nd samples were measured in static mode and the
24 $^{143}\text{Nd}/^{144}\text{Nd}$ values were corrected internally for fractionation by using $^{146}\text{Nd}/^{144}\text{Nd} = 0.7219$
25 (O'Nions et al., 1979) and assuming exponential fractionation behaviour. Measurements of the Nd

1 international standard JNdi yielded a value of $^{143}\text{Nd}/^{144}\text{Nd} = 0.512103 \pm 10$ (2σ) compared with the
2 published value of 0.512115 ± 7 (2σ) (Tanaka et al., 2000). The ϵNd values were calculated using
3 the present-day chondritic uniform reservoir (CHUR) value of 0.512638 for $^{143}\text{Nd}/^{144}\text{Nd}$ (Jacobsen
4 and Wasserburg, 1984).

5

6 **4. Petrography**

7 **4.1. Kaniapiskau Supergroup**

8 The metasedimentary rocks of the Kaniapiskau Supergroup were subdivided into four
9 terrigenous lithotypes based on modal proportions. Lithotypes characterized by greater
10 compositional and textural sedimentary maturity are classified as quartz arenites and subarkoses,
11 and lithotypes with medium to low textural maturity are classified as feldspathic wackes and
12 mudrocks (Fig. 4 and Table 1).

13 Framework grains in the poorly sorted metarenites consist predominantly of rounded to
14 sub-rounded monocrystalline quartz (6.5-100%) with a blue aspect in hand samples and typical
15 undulose extinction under the microscope. Polycrystalline quartz (up to 75%) is sub-rounded to
16 sub-angular, and it often exhibits deformation by diagenetic/metamorphic compaction and
17 breakdown with recrystallization as quartz cement within the framework (Figs. 5A and B).

18 Other monomineralic framework grains include, sub-angular feldspars, predominantly
19 plagioclases (up to 9.3%, An_{27-45}), and minor perthitic alkali feldspar grains (up to 4.6%) with no
20 evident twinning. Two samples are characterized by higher K-feldspar content (up to 22% in 093-
21 A01; Baby Formation, and RP-2298; Denault Formation). One sample from the Baby Formation
22 (coarse-grained metarenite RP-2292-B) shows a relative increase in lithic fragments from
23 metasedimentary (schist and quartzite), granitic and intermediate rocks.

24 The feldspathic wackes and mudrocks record higher compositional maturity, with the
25 exception for one feldspar-rich sample (RP-2261 A1), with poorer matrix content (up to 18%). One

9

1 particular sample (CB-1093 A) contains abundant porphyroblastic biotites, tourmalines and very-
2 fine detrital zircons.

3

4 **4.2. Laporte Group**

5 The Laporte Group (Grand Rosoy and Deborah formations) includes more homogeneous
6 strata characterized by meta-feldspathic and meta-lithic wackes, with variable amounts of matrix
7 (Fig. 4). Considering the post-depositional processes that affected these rocks during diagenesis
8 and metamorphism, an uncertainty of >15% is assigned to the estimated modal proportions of
9 matrix due to the growth of idioblastic muscovite and secondary carbonate during metamorphism.

10 Most Laporte Group samples have at least two metamorphic fabrics and metamorphic
11 minerals such as lepidoblastic biotite, and rare garnet porphyroblasts with pressure shadows
12 indicating syn-tectonic metamorphism. Retrograde parageneses are characterized by thin rims of
13 chlorite and muscovite (Fig. 5C and D) on biotite. Accessory phases are represented by idiomorphic
14 tourmaline, rutile, and allanite with overgrowths of epidote.

15 Very few minerals still preserve the original sedimentary petrofabric, including K-feldspar
16 (Or_{92-95}) with typical microcline twinning and albite (Ab_{78-92}) with remarkable alteration
17 (sericitization) and myrmekite textures.

18 Metamorphosed psephitic rocks within the Grand Rosoy Formation comprise polymictic
19 matrix-supported conglomerates. The granitic clast population are mainly cobble and boulder size,
20 with petrographic variations from quartz-rich leucogranodiorite to quartz-rich alkali-feldspar
21 leucogranite (Figs. 6A to D). Additional sources are indicated by the presence of clasts of hematite-
22 bearing iron formation (Fig. 6E and F).

23

1 **5. Geochemistry**

2 The geochemical signature of sedimentary protoliths can be preserved in high-grade
3 conditions, if significant melt extraction did not occur, because of the low mobility of most major
4 and trace elements during metamorphism (e.g., Cioffi et al., 2012). However, element mobility has
5 been documented during the burial diagenesis of siliciclastic mudstones. For example, K₂O addition
6 and CaO loss is correlated with the progressive illitization of smectite and with the dissolution of
7 calcite. Addition of up to 20% Na₂O in some rocks may be caused by albitization of plagioclase
8 (Wintsch and Kvale, 1994).

9 A chemical classification based on major elements (Herron, 1988) correlates well with
10 petrography (Fig. 7). However, three Kaniapiskau Supergroup samples that classify as
11 sublitharenite on a Log(Fe₂O₃/K₂O) versus Log(SiO₂/Al₂O₃) diagram disagree with the
12 petrographic classification of subarkose (Fig.4). This may be due to the higher iron content of these
13 rocks, which are stratigraphically correlated with banded iron formations in the Ferriman Group.
14

15 **5.1. Comparison between Kaniapiskau Supergroup and Laporte Group rocks**

16 In general, rocks from the Kaniapiskau Supergroup and Laporte Group do not differ
17 significantly in terms of major and trace elements for similar SiO₂ contents (e.g., normal wackes).
18 However, the Laporte Group rocks are more enriched in Sr (median; Kaniapiskau Supergroup = 40
19 ppm; Laporte Group = 242 ppm) and U (median; Kaniapiskau Supergroup = 1.1 ppm; Laporte
20 Group = 2.4 ppm). Rocks from the Kaniapiskau Supergroup also have a large variation of SiO₂ and
21 Al₂O₃ contents (SiO₂/Al₂O₃ = 3.7-51) compared to the more restricted range in Laporte Group rocks
22 (SiO₂/Al₂O₃ = 4.4-6.8) (Supplementary Data I).

23 The rocks from the Laporte Group are enriched in REE compared to those from the
24 Kaniapiskau Supergroup (Σ REE= 236 versus 80) and the REE profiles are less fractionated
25 (La_N/Yb_N= 5.3 versus 15) with stronger negative Eu anomalies (on average, 0.31 versus 0.83

1 respectively) (Fig. 8). All variations in REE are within the range of the main varieties of granitic
2 clasts in metaconglomerates of the Grand Rosoy Formation. The relative Eu enrichment in
3 metawackes of the Deborah Formation compared to the metaconglomerate clasts (average Eu/Eu^*
4 of 0.66 versus 0.32, respectively) could reflect feldspar accumulation and/or mixing with additional
5 sources.

6 In general, the geochemical variations in the Grand Rosoy and Deborah formations fall
7 within the range of the main clast varieties. However, the higher TiO_2 , P_2O_5 , MgO and Ni contents
8 and the high Cr/Th , Co/Ba , Th/U and Rb/Sr ratios in the Deborah Formation suggest the presence
9 of additional mafic/intermediate sources that were not preserved as lithic fragments (Fig. 9).

10

11 **6. Sm-Nd isotope data from matrix-rich metasedimentary rocks and granitic clasts**

12 The calculation of the initial Nd isotope compositions ($\epsilon\text{Nd}_{(t)}$) are based on the
13 sedimentation ages of the different units. The best estimate of a sedimentation age for the second
14 cycle of the Kaniapiskau Supergroup was obtained from rhyolites of the Doublet Group that were
15 dated at 1870 ± 4 Ma (Machado et al., 1997). However, there is no minimum age of sedimentation
16 for the volcanic rocks within the Laporte Group, so we used the maximum age of 1834 ± 2.4 Ma,
17 determined from the detrital zircon population (Henrique-Pinto et al., 2017). The time between
18 maximum and minimum age of sedimentation was likely relatively short as metamorphism of the
19 Laporte Group began as early as 1793 ± 2 Ma (U-Pb monazite; Machado et al., 1989).

20 Previously, the only Sm-Nd isotope data for sedimentary rocks of the Labrador Trough
21 were three samples from the Baby Formation of the Kaniapiskau Supergroup (Dia et al., 1990),
22 although only one sample yielded an unperturbed depleted mantle model age (Nd TDM) of 2.8 Ga
23 and an $\epsilon\text{Nd}_{(1.87 \text{ Ga})}$ value of -10.

24 New Sm-Nd isotope data for the Kaniapiskau Supergroup were obtained from two samples
25 from the Baby Formation, two metabasalts from the Hellancourt Formation and one metagabbro

1 from the Montagnais Sills. The results span approximately the same TDM range indicated by the
2 earlier work (2.7 to 3.2 Ga), although the ϵNd values of the Baby Formation samples are slightly
3 more negative (-12).

4 The metabasalt samples from the Hellancourt Formation yielded important differences. The
5 sample from the western part of the Kaniapiskau Supergroup (CB-1024) has a slightly negative
6 $\epsilon\text{Nd}_{(1.87\text{ Ga})}$ value of -2.3, in contrast to the pillow basalt (RP-2301) from the eastern part that yielded
7 a juvenile $\epsilon\text{Nd}_{(1.87\text{ Ga})}$ value of +3.3.

8 The subvolcanic Montagnais sample (CB-1102) also has a slightly negative $\epsilon\text{Nd}_{(1.87\text{ Ga})}$
9 value (-1.9) and, like the metabasalt from the eastern part of Kaniapiskau Supergroup, yielded an
10 older TDM age (>2.7 Ga).

11 The ϵNd variation in metawackes from the Grand Rosoy Formation ($\epsilon\text{Nd}_{(1.83\text{ Ga})}$ -0.1 to
12 +2.8) overlap the compositions ($\epsilon\text{Nd}_{(1.83\text{ Ga})}$ +2.9 to +3.2) from the main varieties of juvenile granitic
13 clasts from metaconglomerates of the same formation. In contrast, rocks from the Deborah
14 Formation have negative $\epsilon\text{Nd}_{(1.83\text{ Ga})}$ values (-4.4 to -9.1), suggesting a contribution from more
15 evolved sources with TDM ages between 2.7 and 2.8 Ga (Fig. 10).

16

17 **7. Inferences on tectonic environment**

18 Rocks with high compositional and textural sedimentary maturity, such as the quartz
19 arenites and subarkoses of the Kaniapiskau Supergroup, are typical of a craton interior and
20 transitional continental settings (e.g., Dickinson, 1985). The elevated iron contents for some
21 samples of the Denault and Baby formations resemble iron formation units within the Ferriman
22 Group, supporting the interpretation that they are stratigraphically associated (e.g., Wardle et al.,
23 1990; Clark et al., 2008; Zentmyer et al., 2011; Henrique-Pinto et al., 2017).

24 In contrast, rocks from the Laporte Group represent a more homogeneous group of
25 feldspathic and lithic wackes with variable matrix contents with quartz cement and secondary

1 metamorphic minerals such as idioblastic muscovite and secondary carbonate. Given the overprint
2 of the sedimentary petrofabric, a geotectonic QFL-diagram is not applicable (see discussion in Cox
3 and Lowe, 1996).

4 The plot of Laporte Group samples on a K_2O/Na_2O vs. SiO_2 diagram (Roser and Korsh,
5 1986) suggests a depositional setting typical of an active continental margin (Fig.11). Thus, the
6 Laporte Group metaconglomerates should contain, in addition to the dominant felsic granitic clasts,
7 fine-grained, volcanic sedimentary detritus (Fig. 12).

8 As already indicated by a detrital zircon provenance study (Henrique-Pinto et al., 2017)
9 the presence of matrix-rich metasedimentary rocks in the Grand Rosoy Formation and juvenile
10 granitic clasts with slightly negative to positive $\epsilon Nd_{(1.83 Ga)}$ values in the metaconglomerates is
11 consistent with an andesitic arc-related sedimentary basin (Fig. 13). However, the lower $\epsilon Nd_{(1.83}$
12 $Ga)}$ values (-4.4 to -9.1) in metawackes of the Deborah Formation suggest a contribution from older
13 (> 1.8 Ga) crustal components (Figs. 13 and 14).

14 Four Kaniapiskau Supergroup samples record significant diagenetic/metamorphic
15 albitization with the introduction of secondary carbonates, which hinders the interpretation of its
16 tectonic setting through the use of major element discriminant diagrams (Fig. 11). Nevertheless,
17 the abundance of recycled mature polycyclic detritus in the Kaniapiskau Supergroup rocks is
18 consistent with an intraplate continental margin environment and negative ϵNd values suggest that
19 the sediment provenance included Paleoproterozoic sources.

20

21 **8. Discussion**

22 The Laporte Group has been considered a high-grade metamorphic equivalent of some
23 formations within the Kaniapiskau Supergroup since the 1950s (e.g., Harrison, 1952; Taylor, 1979;
24 Wardle et al., 2002; Wardle and Bailey, 1981; Poirier et al., 1990; Girard, 1995). However, in light
25 of the differences in their detrital zircon populations (Henrique-Pinto et al., 2017), it is unlikely that

1 the metasedimentary rocks of the Kaniapiskau Supergroup and the Laporte Groupe received
2 terrigenous material from the same source. This conclusion is also supported by contrasting
3 geochemical signatures. For example, the Laporte Group rocks have higher REE enrichment with
4 less fractionated patterns and slightly negative Eu anomalies compared to Kaniapiskau Supergroup
5 rocks.

6 First cycle sedimentation within the Kaniapiskau Supergroup began in an intracontinental
7 rift-related environment (Clark and Wares 2005; Fig. 15-A) and Hoffman (1987, 1988, 1990a)
8 proposed a foreland model for the second cycle of sedimentation of the Kaniapiskau Supergroup.
9 However, the foreland model is difficult to reconcile with an age-gap of more than 150 Ma between
10 the crystallization and depositional ages of the detrital zircon population from the Denault and Baby
11 formations. The age-gap is more consistent with those of detrital zircons from passive continental
12 margins (Henrique-Pinto et al., 2017). This hypothesis is corroborated by the Sm-Nd isotope data
13 of this study that indicates sediment sources derived exclusively from Paleoproterozoic terrains (TDM
14 3.2 Ga; $\epsilon\text{Nd} = -12.$) (Fig. 15-B).

15 The metabasalt from the western part of the Kaniapiskau Supergroup records a slightly
16 negative $\epsilon\text{Nd}_{(1.88 \text{ Ga})}$ value (-2.3) that could indicate that the magmas were contaminated by
17 assimilation of sedimentary rocks within the passive margin. In contrast, pillow basalt from the
18 eastern part of the Kaniapiskau Supergroup yields a positive $\epsilon\text{Nd}_{(1.87 \text{ Ga})}$ value (+3.3) that is
19 consistent with a depleted MORB-like ocean floor spreading eastward, as has been suggested by
20 some authors (e.g., Van der Leeden et al., 1990; Boone and Hynes, 1990). More robust conclusions
21 would require further investigation.

22 Two main formations of the Laporte Group (Girard, 1995) are the Grand Rosoy formation
23 (basal), including polymictic metaconglomerates, and Deborah Formation (upper unit), which
24 records higher TiO_2 , P_2O_5 , MgO and Ni contents and high Cr/Th, Co/Ba, Th/U and Rb/Sr ratios.

1 These features suggest the presence of additional sediment sources that were probably of
2 mafic/intermediate composition and were not preserved as lithic fragments.

3 Van der Leeden et al. (1990) proposed that the Kaniapiskau Supergroup coexisted eastward
4 with a forearc accretionary wedge (Laporte Group) bordering the De Pas Batholith in an Andean-
5 type magmatic arc environment. Henrique-Pinto et al. (2017) proposed that <100 Ma age-gap
6 between the crystallization and depositional ages for the detrital zircon population within the Grand
7 Rosoy Formation is consistent with detrital zircon provenance recognized in forearc settings and
8 the Andean-type magmatic arc model. The positive $\epsilon\text{Nd}_{(1.83 \text{ Ga})}$ values of the matrix-rich
9 metasedimentary rocks and juvenile granitic clasts in metaconglomerates of the Grand Rosoy
10 Formation are also consistent with deposition in a continental forearc setting, with exposed and
11 dissected early-arc infrastructure (Fig. 15-C).

12 The development of a forearc basin (and its basement) in modern orogens is followed by
13 crustal thickening with the development of a wedge-top depozone in the upper plate during the
14 continental collision phase. Examples of this evolution are found in the southern Taiwan foreland
15 basin (Chiang et al., 2004; Malavieille and Trullenque, 2009) and the Himalayan Orogen in
16 southwestern Tibet (Wang et al., 2015).

17 Following this model, the Deborah Formation would have been deposited above the forearc
18 basin and the model is consistent with the detrital zircon age pattern of the Deborah Formation
19 (Henrique-Pinto et al., 2017) (Fig. 15-D). The negative $\epsilon\text{Nd}_{(1.83 \text{ Ga})}$ values (-4.4 to -9.1) from the
20 Deborah formation suggest a contribution from more evolved sources, possibly derived from the
21 passive margin exposed in the accretionary wedge, and from exposed crustal levels of the Core
22 Zone terrane.

1 **9. Concluding remarks**

2 The petrography, geochemistry and Sm-Nd isotopic data of matrix-rich conglomerates,
3 wackes and mudrocks were used as provenance tools to characterize the tectonic settings of the
4 Labrador Trough. The following conclusions can be drawn from our study:

5

6 (i) Rocks from the Kaniapiskau Supergroup have geochemical and isotopic signatures akin to
7 cratonic interior and transitional continental paleo-environments, and record greater compositional
8 maturity, with a wide range of textural maturity that is typical of an intraplate continental margin
9 basin;

10

11 (ii) Compared to the Kaniapiskau Supergroup, the Laporte Group rocks have less fractionated REE
12 patterns and slight negative Eu anomalies, which supports the interpretation that metasedimentary
13 rocks of the Kaniapiskau Supergroup and Laporte Group received terrigenous material from
14 different source areas;

15

16 (iii) The higher TiO_2 , P_2O_5 , MgO and Ni contents and high Cr/Th, Co/Ba, Th/U and Rb/Sr ratios
17 of the Deborah Formation suggest the presence of additional mafic/intermediate sources during
18 deposition;

19

20 (iv) Nd isotopes of matrix-rich metasedimentary rocks and juvenile granitic clasts within
21 metaconglomerates of the Grand Rosoy Formation (Laporte Group) are consistent with an arc-
22 related sedimentary environment, possibly a continental forearc with juvenile dissected early-arc
23 substrate as the main source area; and

24

1 (v) As expected in a collisional pro-foreland basin especially in a wedge-top depozone, the
2 sedimentary record of the Deborah Formation (Laporte Group) includes contributions that were
3 probably derived from the passive margin exposed in the accretionary wedge and eroded crustal
4 levels of the Core Zone terrane.

5

6 **Acknowledgements**

7 A post-doctoral scholarship to RHP supported by the MERNQ (grant - 8449-2017-2018-
8 14). Additional support came from an NSERC-Discovery grant to CG and RS. The authors
9 acknowledge the meticulous technical support provided by André Poirer and Julien Gogot. The
10 authors also acknowledge the efficient way in which the manuscript was handled by Dr. Ali Polat
11 (Editor) and the careful reviews and suggestions provide by Dr. Luke Beranek (Associate Editor),
12 Dr. Darrel G.F. Long and other two anonymous reviewers that helped improve the manuscript.

13

14 **References**

- 15 Baragar, W.R.A. 1967. Wakuach Lake map-area, Quebec-Labrador (23 O). Geological Survey of
16 Canada, Memoir 344, 174 p.
- 17 Bhatia, M.R. 1985. Rare earth element geochemistry of australian paleozoic graywackes and
18 mudrocks: provenance and tectonic control. *Sediment. Geol.*, 45: 97-113.
- 19 Biševac, V., Krenn, E., Balen, D., Finger, F., Balogh, K. 2011. Petrographic, geochemical and
20 geochronological investigation on granitic pebbles from Permotriassic metasediments of
21 the Tisia terrain (eastern Papuk, Croatia). *Miner Petrol* (2011) 102:163–180.
- 22 Boon, E. and Hynes, A. 1990. A structural cross-section of the northern Labrador Trough, New
23 Quebec. *The Early Proterozoic Trans-Hudson Orogen*. Edited by JF Lewry and MR
24 Stauffer. Geological Association of Canada, Special Paper, 37, 387-396.

- 1 Chauvel, J.J. and Dimroth, E. 1974. Facies types and depositional environment of the Sokoman iron
2 formation, Central Labrador Trough, Quebec, Canada. *Journal of Sedimentary Petrology*,
3 44(2), 299-327.
- 4 Charette, B., Lafrance, I., Mathieu, G. 2016. Géologie de la région du lac Jeannin (SNRC 24B).
5 Ministère de l'Énergie et des Ressources naturelles, Québec.
- 6 Chiang, C.S., Yu, H.S., Chou, Y.W. 2004. Characteristics of the wedge-top depozone of the southern
7 Taiwan foreland basin system. *Basin Research*, 16(1), 65-78.
- 8 Cioffi, C.R., Campos Neto, M.C., Rocha, B.C., Moraes, R., Henrique-Pinto, R. 2012. Geochemical
9 signatures of metasedimentary rocks of high-pressure granulite facies and its relation with
10 partial melting: Carvalhos Klippe, Southern Brasilia Belt, Brazil. *Journal of South
11 America Earth Sciences* 40, 63-73.
- 12 Clark, T. 1988. Stratigraphie, pétrographie et pétrochimie de la formation de fer de Baby dans la
13 région du lac Hérodier (Fossa du Labrador). Ministère de l'Énergie et des Ressources,
14 Québec, ET 87-13, 36p.
- 15 Clark, T. and Wares, R. 2005. Lithotectonic and metallogenic synthesis of the New Québec Orogen
16 (Labrador Trough). *Ministère des Ressources Naturelles et Faune, MM*, 1, 180p.
- 17 Clark, T., Leclair, A., Pufahl, P., David, J. 2008. Recherche géologique et métallogénique dans les
18 régions de Schefferville (23J15) et du lac Zeni (23I16). Ministère des Ressources
19 naturelles et de la Faune, Québec, 2008-01.
- 20 Corrigan, D., Pehrsson, S., Wodicka, N., De Kemp, E. 2009. The Palaeoproterozoic Trans-Hudson
21 Orogen: a prototype of modern accretionary processes. *Geological Society, London*,
22 *Special Publications*, 327(1), 457-479.
- 23 Cox, R.N., Lowe, D.R. and Cullers, R.L. 1995. The influence of sediment recycling and basement
24 composition on evolution of mudrock chemistry in the southwestern United States.
25 *Geochimica et Cosmochimica Acta*, 59(14): 2919-2940.

- 1 De Paolo D.J. 1988. Neodymium isotope geochemistry: an introduction. In: Minerals and rocks, vol.
2 20, Springer, New York, p 187.
- 3 Dickinson, W.R. 1985. Interpreting provenance relations from detrital modes of sandstones. In: G.G.
4 Zuffa (ed.). Provenance of Arenites. by D. Reidel Publishing Company: 333-361.
- 5 Dimroth, E. and Chauvel, J.J. 1973. Petrography of the Sokoman iron formation in part of the central
6 Labrador trough, Quebec, Canada. Geological Society of America Bulletin, 84(1), 111-
7 134.
- 8 Eaton, D.W. and Darbyshire, F. 2010. Lithospheric architecture and tectonic evolution of the
9 Hudson Bay region. Tectonophysics, 480(1), 1-22.
- 10 Fahrig, W.F. 1952. Griffis Lake (west Half) Quebec. Geological Survey of Canada. Paper 51-23.
- 11 Frarey, M.J. and Duffell, S. 1964. Revised stratigraphic nomenclature for the central part of the
12 Labrador Trough. Geological Survey of Canada, 64-25, 1-12.
- 13 Gélinas, L. 1965. Géologie de la région de Fort Chimo et des lacs Gabriel et Thévenet, Nouveau-
14 Québec. Thèse de doctorat, Université Laval, Québec, 212 pages.
- 15 Girard, R. 1995. Geologie de la region du lac Deborah, Territoire-du-Nouveau-Quebec. Ministere
16 des Ressources naturelles, Quebec MB 95-20, 177p.
- 17 Harrison, J.M. 1952. The Quebec-Labrador Iron Belt, Quebec and Newfoundland: Preliminary
18 Report. Geological Survey of Canada, Department of Mines and Technical Surveys, Paper
19 52-20, 1-20.
- 20 Henrique-Pinto, R., Janasi, V.A., Simonetti, A., Tassinari, C.C.G., Heaman, L.M., 2012.
21 Paleoproterozoic source contributions to the São Roque Group sedimentation: LA-MC-
22 ICPMS U-Pb dating and Sm-Nd systematics of clasts from metaconglomerates of the
23 Boturuna Formation. Geologia USP, 12(3), 21-32.
- 24 Henrique-Pinto, R., Janasi, V.A., Tassinari, C.C.G., Carvalho, B.B., Cioffi, C.R., Stríkis, N.M. 2015.
25 Provenance and sedimentary environments of the Proterozoic São Roque Group, SE-

- 1 Brazil: Contributions from petrography, geochemistry and Sm–Nd isotopic systematics of
2 metasedimentary rocks. *Journal of South American Earth Sciences*, 63, 191-207.
- 3 Henrique-Pinto, R., Janasi, V.A., Vasconcellos, A.C.B.C., Sawyer, E.W., Barnes, S.-J., Basei,
4 M.A.S., Tassinari, C.C.G. 2015. Zircon provenance in meta-sandstones of the Sao Roque
5 Domain: implications for the Proterozoic evolution of the Ribeira Belt, SE Brazil,
6 *Precambrian Research*, 256, 271-288.
- 7 Henrique-Pinto, R., Guilmette, C., Bilodeau, C., McNicoll, V. 2017. Evidence for transition from a
8 continental forearc to a collisional pro-foreland basin in the eastern Trans-Hudson Orogen:
9 detrital zircon provenance analysis in the Labrador Trough, Canada. *Precambrian
10 Research*, 296, 181-194.
- 11 Herron, M.M. 1988. Geochemical classification of terrigenous sands and shales from core or log
12 data. *Journal of Sedimentary Research*. 58(5), 820-829.
- 13 Hoffman, E.L. 1992. Instrumental Neutron Activation in Geoanalysis. *Journal of Geochemical
14 Exploration*, v. 44, pp. 297-319.
- 15 Hoffman, P.F. 1987. Early Proterozoic Foredeeps, Foredeep Magmatism, and Superior - Type Iron
16 - Formations of the Canadian Shield. *Proterozoic Lithospheric Evolution*, 85-98.
- 17 Hoffman, P.F. 1988. United Plates of America, the birth of a craton-Early Proterozoic assembly and
18 growth of Laurentia. *Annual Review of Earth and Planetary Sciences*, 16, 543-603.
- 19 Hoffman, P.F. 1990a. Subdivision of the Churchill Province and extent of the Trans-Hudson
20 Orogen. *In: The Early Proterozoic Trans-Hudson Orogen of North America*. Edited by JF
21 Lewry and MR Stauffer. Geological Association of Canada, Special Paper, 37, 15-39.
- 22 Hoffman, P.F. 1990b. Dynamics of the tectonic assembly of northeast Laurentia in geon 18 (1.9-1.8
23 Ga). *Geoscience Canada*, 17(4), 222-226.
- 24 Jacobsen, S.B., Wasserburg, G.J., 1984. Sm–Nd isotopic evolution of chondrites and achondrites.
25 *Earth Planet. Sci. Lett.* 67, 137-150.

- 1 James, D.T., Connelly, J.N., Wasteneys, H.A., Kilfoil, G.J. 1996. Paleoproterozoic lithotectonic
2 divisions of the southeastern Churchill Province, western Labrador. *Canadian Journal of*
3 *Earth Sciences*, 33(2), 216-230.
- 4 James, D.T. and Dunning, G.R. 2000. U-Pb geochronological constraints for Paleoproterozoic
5 evolution of the core zone, southeastern Churchill Province, northeastern Laurentia.
6 *Precambrian Research*, 103(1), 31-54.
- 7 Klein, C. and Fink, R.P. 1976. Petrology of the Sokoman Iron Formation in the Howells River area,
8 at the western edge of the Labrador Trough. *Economic Geology*, 71(2), 453-487.
- 9 Lewry, J.F. and Collerson, K.D. 1990. The Trans-Hudson Orogen: extent, subdivision, and
10 problems. In: *The Early Proterozoic Trans-Hudson Orogen of North America*. Edited by
11 JF Lewry and MR Stauffer. Geological Association of Canada, Special Paper, 37, 1-14.
- 12 Machado, N., Goulet, N., Gariépy, C. 1989. U-Pb geochronology of reactivated Archean basement
13 and of Hudsonian metamorphism in the northern Labrador Trough. *Canadian Journal of*
14 *Earth Sciences*, 26(1), 1-15.
- 15 Machado, N. 1990. Timing of collisional events in the Trans-Hudson Orogen: evidence from U-Pb
16 geochronology for the New Quebec Orogen, the Thompson Belt, and the Reindeer Zone
17 (Manitoba and Saskatchewan). In: *The Early Proterozoic Trans-Hudson Orogen of North*
18 *America*. Edited by JF Lewry and MR Stauffer. Geological Association of Canada, Special
19 Paper, 37, 433-441.
- 20 Machado, N., Clark, T., David, J., Goulet, N. 1997. U-Pb ages for magmatism and deformation in
21 the New Quebec Orogen. *Canadian Journal of Earth Sciences*, 34(5), 716-723.
- 22 Malavieille, J. and Trullenque, G. 2009. Consequences of continental subduction on forearc basin
23 and accretionary wedge deformation in SE Taiwan: Insights from analogue modeling.
24 *Tectonophysics*, 466(3), 377-394.

- 1 McLennan, S.M., Hemming, S.R. 1991. Samarium/neodymium elemental and isotopic systematics
2 in sedimentary rocks. *Geochimica et Cosmochimica Acta*, 56, 887-898.
- 3 McLennan, S.M., Taylor, S.R., McCulloch, M.T., Maynard, J.B. 1990. Geochemical and Nd-Sr
4 isotopic composition of deep-sea turbidites: Crustal evolution and plate tectonic
5 associations. *Geochimica et Cosmochimica Acta*, 54, 2015-2050.
- 6 McLennan, S.M., Hemming, S.R., Taylor, S.R., Eriksson, K.A. 1995. Early Proterozoic crustal
7 evolution: Geochemical and Nd-Pb isotopic evidence from metasedimentary rocks,
8 southwestern North America. *Geochimica et Cosmochimica Acta*, 59(6): 1153-1177.
- 9 McLennan, S.M., Hemming, S., McDaniel, D.K., and Hanson, G.N. 1993. Geochemical approaches
10 to sedimentation, provenance, and tectonics, in Johnsson, M.J. and Basu, A. eds.,
11 Processes Controlling the Composition of Clastic Sediments: Boulder, Colorado,
12 Geological Society of America Special Paper 284.
- 13 Melezhik, V., Fallick, A. and Clark, T. 1997. Two billion year old isotopically heavy carbon:
14 evidence from the Labrador Trough, Canada. *Canadian Journal of Earth Sciences*, 34(3),
15 271-285.
- 16 Meert, J.G. 2012. What's in a name? The Columbia (Paleopangaea/Nuna) supercontinent.
17 *Gondwana Research*, 21(4), 987-993.
- 18 Naqvi, S.M., Divakara Rao, V., Hussain, S.M., Naraya, B.L. 1978 The petrochemistry and geologic
19 implications of conglomerates from Archaean geosynclinal piles of southern India. *Can.*
20 *J. Earth Sci.* v. 15, 1085-1100.
- 21 Nesbitt, H.W. and Young, G.M. 1982. Early Proterozoic climates and plate motions inferred from
22 major element chemistry of lutites. *Nature*, 299, 715-717.
- 23 Nesbitt, H.W. and Young, G.M. 1996. Petrogenesis of sediments in the absence of chemical
24 weathering: effects of abrasion and sorting on bulk composition and mineralogy.
25 *Sedimentology*, 43, 341-358.

- 1 Nesbitt, H.W., Young, G.M., McLennan, S.M., Keays, R.R. 1996. Effects of Chemical Weathering
2 and Sorting on the Petrogenesis of Siliciclastic Sediments, with Implications for
3 Provenance Studies. *The Journal of Geology*, 104(5), 525-542.
- 4 Nichols, G. 2009. *Sedimentology and stratigraphy*. John Wiley & Sons.
- 5 O'Nions, R.K., Carter, S.R., Evensen, N.M., Hamilton, P.J. 1979. Geochemical and Cosmochemical
6 Applications of Nd Isotope Analysis. *Annual Review of Earth and Planetary Sciences* (7),
7 11-38.
- 8 Pettijohn, F.J. 1975. *Sedimentary Rocks* (3rd edition). Harper and Row, New York.
- 9 Poirier, G., Perreault, S., Hynes, A. 1990. Nature of the eastern boundary of the Labrador Trough
10 near Kuujuaq, Quebec. In: *The Early Proterozoic Trans-Hudson Orogen*. Edited by JF
11 Lewry and MR Stauffer. Geological Association of Canada, Special Paper, 37, 397-412.
- 12 Reimer, T., Condie, K., Schneider, G., Georgi, A. 1985. Geochemistry of granitoid and
13 metamorphic pebbles from the early Archean Moodies Group, Barberton
14 Mountainland/South Africa. *Precambrian Research*, 29: 383-404.
- 15 Rogers, J.J. and Santosh, M. 2002. Configuration of Columbia, a Mesoproterozoic supercontinent.
16 *Gondwana Research*, 5(1), 5-22.
- 17 Rohon, M.L., Vialette, Y., Clark, T., Roger, G., Ohnenstetter, D., Vidal, P. 1993. Apebian mafic-
18 ultramafic magmatism in the Labrador Trough (New Quebec): its age and the nature of its
19 mantle source. *Canadian Journal of Earth Sciences*, 30(8), 1582-1593.
- 20 Roser, B.P. and Korsch, R.J. 1986. Determination of tectonic setting of sandstone-mudstone suites
21 using content and ratio. *The Journal of Geology*, 94(5), 635-650.
- 22 Roser, B.P. and Korsch, R.J. 1988. Provenance signatures of sandstone-mudstone suites determined
23 using discriminant function analysis of major-element data. *Chemical Geology*, 67, 119-
24 139.

- 1 Simard, M., Lafrance, I., Hammouche, H., Legoux, C. 2013. Géologie de la région de Kuujjuaq et
2 de la baie d'Ungava (SRNC 24J, 24K). Ministère des Ressources Naturelles, Québec, RG,
3 4, 60.
- 4 Stauffer, M.R. 1984. Manikewan: an early Proterozoic ocean in central Canada, its igneous history
5 and orogenic closure. *Precambrian Research*, 25(1), 257-281.
- 6 Tanaka, T., Togashi, S., Kamioka, H., Amakawa, H., Kagami, H., Hamamoto, T., Yuhara, M.,
7 Orihashi, Y., Yoneda, S., Shimizu, H., Kunimaru, T., Takahashi, K., Yanagi, T., Nakano,
8 T., Fujimaki, H., Shinjo, R., Asahara, Y., Tanimizu, M., and Dragusanu, C. 2000. JNdi-1:
9 a neodymium isotopic reference in consistency with LaJolla neodymium. *Chemical
10 Geology*, 168(3-4): 279–281. doi:10.1016/S0009-2541(00)00198-4.
- 11 Taylor, F.C. 1979. Reconnaissance geology of a part of the Precambrian Shield, northeastern
12 Quebec, northern Labrador and Northwest Territories. Geological Survey of Canada,
13 Memoir 393.
- 14 Taylor, S.R. and McLennan, S.M. 1985. *The Continental Crust: Its Composition and Evolution*.
15 Blackwell. 298p.
- 16 Wang, J.G., Hu, X.M., BouDagher-Fadel, M., Wu, F.Y., Sun, G.Y. 2015. Early Eocene sedimentary
17 recycling in the Kailas area, southwestern Tibet: Implications for the initial India–Asia
18 collision. *Sedimentary Geology*, 315, 1-13.
- 19 Wardle, R.J. and Bailey, D.G. 1981. Early Proterozoic sequences in Labrador. In: Campbell, F.H.A.,
20 ed., *Proterozoic Basins of Canada*. Geological Survey of Canada, paper 81-10, 331-358.
- 21 Wardle, R.J., Ryan, B., Nunn, G.A.G., Mengel, F.C. 1990. Labrador segment of the Trans-Hudson
22 Orogen: crustal development through oblique convergence and collision. In: *The Early
23 Proterozoic Trans-Hudson Orogen of North America*. Edited by JF Lewry and MR
24 Stauffer. Geological Association of Canada, Special Paper, 37, 353-369.

- 1 Wardle, R.J., James, D.T., Scott, D.J., Hall, J. 2002. The southeastern Churchill Province: synthesis
2 of a Paleoproterozoic transpressional orogen. *Canadian Journal of Earth Sciences*, 39(5),
3 639-663.
- 4 Wintsch, R.P., Kvale, C.M. 1994. Differential mobility of elements in burial diagenesis of
5 siliciclastic rocks. *Journal of Sedimentary Research*, 64(2a): 349-361.
- 6 Van der Leeden, J., Bélanger, M., Danis, D., Girard, R., Martelain, J. 1990. Lithotectonic domains
7 in the high-grade terrain east of the Labrador Trough (Quebec). In: *The Early Proterozoic*
8 *Trans-Hudson Orogen*. Edited by JF Lewry and MR Stauffer. Geological Association of
9 Canada, Special Paper, 37, 371-386.
- 10 Zentmyer, R.A., Pufahl, P.K., James, N.P., Hiatt, E.E. 2011. Dolomitization on an evaporitic
11 Paleoproterozoic ramp: widespread syndimentary dolomite in the Denault Formation,
12 Labrador Trough, Canada. *Sedimentary Geology*, 238(1), 116-131.
- 13 Zhao, G., Sun, M., Wilde, S.A., Li, S. 2004. A Paleo-Mesoproterozoic supercontinent: assembly,
14 growth and breakup. *Earth-Science Reviews*, 67(1), 91-123.
- 15
- 16

17 **FIGURE CAPTIONS**

18

19 **Fig. 1:** Easternmost part of the Circum-Ungava Belt (modified from Henrique-Pinto et al., 2017).

20 **Fig. 2:** Geological map of the Labrador Trough (north) showing parts of the Kaniapiskau
21 Supergroup and Laporte Group, and the locations of dated samples (modified from
22 <http://sigeom.mines.gouv.qc.ca>).

23 **Fig. 3:** Schematic stratigraphy of the Kaniapiskau Supergroup (modified from Clark and Wares,
24 2005). CC= Castignon Lake Carbonatite Complex.

1 **Fig. 4:** Labrador Trough samples plotted on a QFL ternary diagram: Q=quartz, F=feldspar, L=lithic
2 fragments. Fields after Dott (1964), McBride (1963) and Pettijohn (1975).

3 **Fig. 5:** Photomicrographs of metasedimentary rocks of the Kaniapiskau Supergroup and Laporte
4 Group (left, parallel polarizers; right, crossed polarizers). A- subarkose from the Denault
5 Formation; B- quartz arenite from the Baby Formation; C- feldspathic wacke from the Grand Rosoy
6 Formation; D- quartz wacke from the Deborah Formation. Abbreviations: Qzp%= polycrystalline
7 quartz; Qzm%= monocrystalline quartz; Qt%= total quartz; L%= lithic fragments; Ft%= total feldspars; Kfs=
8 K-feldspar; Pl= plagioclase; Cb= carbonate; Op. min.= opaque minerals; Acc= Accessory.

9 **Fig. 6:** Main clast variety of psephitic rocks from the Grand Rosoy Formation. A- quartz-rich
10 leucocratic granodiorite; B- mesocratic monzogranite; C- leucocratic monzogranite; D- quartz-rich
11 leucocratic alkali-feldspar granite; E and F- hematite-bearing iron formation.

12 **Fig. 7:** Chemical classification diagram [$\log(\text{SiO}_2/\text{Al}_2\text{O}_3)$ versus $\log(\text{Fe}_2\text{O}_3/\text{K}_2\text{O})$] (Herron, 1988)
13 for samples from the Kaniapiskau Supergroup and Laporte Group.

14 **Fig. 8:** Chondrite-normalized (Taylor and McLennan, 1985) rare-earth element patterns for
15 metasedimentary rocks of the Labrador Trough.

16 **Fig. 9:** Trace element variation diagrams versus SiO_2 in metasedimentary rocks of the Laporte
17 Group. Grey shaded areas represent the range of granitic clast compositions.

18 **Fig. 10:** ENd versus TDM (Ga) diagram for metamudrocks and metawackes from the Kaniapiskau
19 Supergroup and Laporte Group. DM = depleted mantle curve from De Paolo (1988).

20 **Fig. 11:** Labrador Trough samples plotted on a $\text{K}_2\text{O}/\text{Na}_2\text{O}$ vs. SiO_2 diagram (Roser and Korsch,
21 1986).

22 **Fig. 12:** Provenance signatures using discriminant function analysis from Roser and Korsch (1988)
23 applied to rocks from the Kaniapiskau Supergroup and Laporte Group. The discriminant functions
24 are:

$$25 \quad F1 = -(1,773 * \text{TiO}_2) + (0,607 * \text{Al}_2\text{O}_3) + (0,76 * \text{Fe}_2\text{O}_3) - (1,5 * \text{MgO}) + (0,616 * \text{CaO}) + (0,509 * \text{Na}_2\text{O}) - (1,224 * \text{K}_2\text{O}) - 9,09;$$

$$26 \quad F2 = (0,445 * \text{TiO}_2) + (0,07 * \text{Al}_2\text{O}_3) - (0,25 * \text{Fe}_2\text{O}_3) - (1,142 * \text{MgO}) + (0,438 * \text{CaO}) + (1,475 * \text{Na}_2\text{O}) + (1,426 * \text{K}_2\text{O}) - 6,861;$$

1 $F1^* = ((30,638 * TiO_2) / Al_2O_3) -$
 2 $(12,541 * Fe_2O_3) / Al_2O_3 + ((7,329 * MgO) / Al_2O_3) + ((12,031 * Na_2O) / Al_2O_3) + ((35,402 * K_2O) / Al_2O_3) - 6,382;$
 3 $F2^* = (((56,5 * TiO_2) / Al_2O_3) - ((10,879 * Fe_2O_3) / Al_2O_3) + ((30,875 * MgO) / Al_2O_3) -$
 4 $((5,404 * Na_2O) / Al_2O_3) + ((11,112 * K_2O) / Al_2O_3) - 3,89).$ Legend as in Figure 10.

5 **Fig. 13:** Plot of ϵNd versus Th/Sc ratio (McLennan et al., 1990) for metamudrocks and metawackes
 6 of the Kaniapiskau Supergroup and Laporte Group.

7 **Fig. 14:** Plot of $f Sm/Nd$ versus ϵNd (McLennan and Hemming, 1991) for metamudrocks,
 8 metawackes and metavolcanic rocks of the Kaniapiskau Supergroup and Laporte Group.

9 **Fig. 15:** Preferred tectonic model for the evolution of the New Quebec Orogen.

10

11 TABLE CAPTION

12

13 **Table 1:** Modal mineralogy of metasedimentary rocks from the Kaniapiskau Supergroup and
 14 Laporte Group. Abbreviations: Qzp%= polycrystalline quartz; Qzm%= monocrystalline quartz;
 15 Qt%= total quartz; L%= lithic fragments; Ft%= total feldspars; Kfs= K-feldspar; Pl= plagioclase;
 16 Cb= carbonate; Op. min.= opaque minerals; Acc= Accessory. *1= quartz arenite; *2= subarkose;
 17 *3= feldspathic wacke and *4= mudrock.

18

19 **Table 2:** Sm-Nd isotope data for metamudstones of the Kaniapiskau Supergroup and Laporte
 20 Group.

21

22 SUPPLEMENTARY DATA

23

24 **Table S1:** Results of chemical analyses on metasedimentary rocks of the Kaniapiskau Supergroup
 25 and Laporte Group.

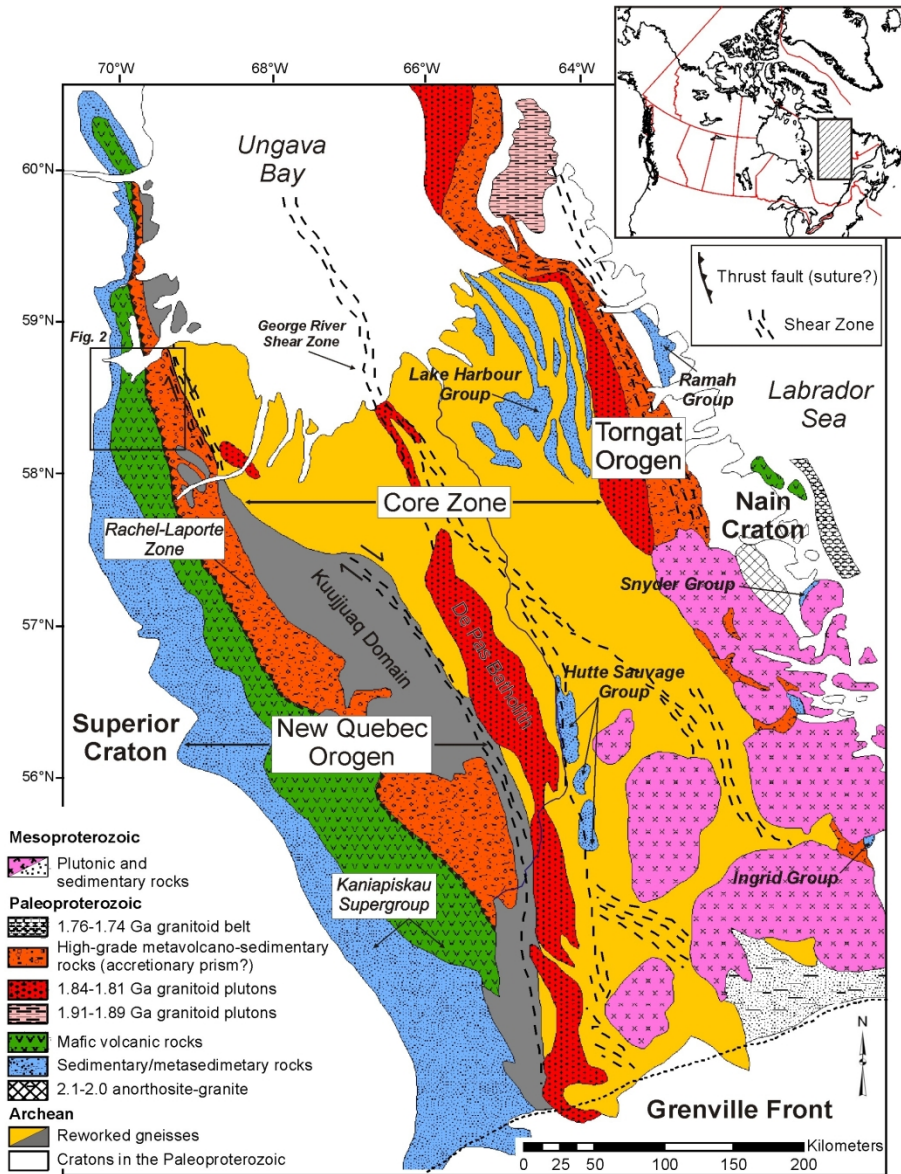


Fig. 1: Easternmost part of the Circum-Ungava Belt (modified from Henrique-Pinto et al., 2017).

182x237mm (300 x 300 DPI)

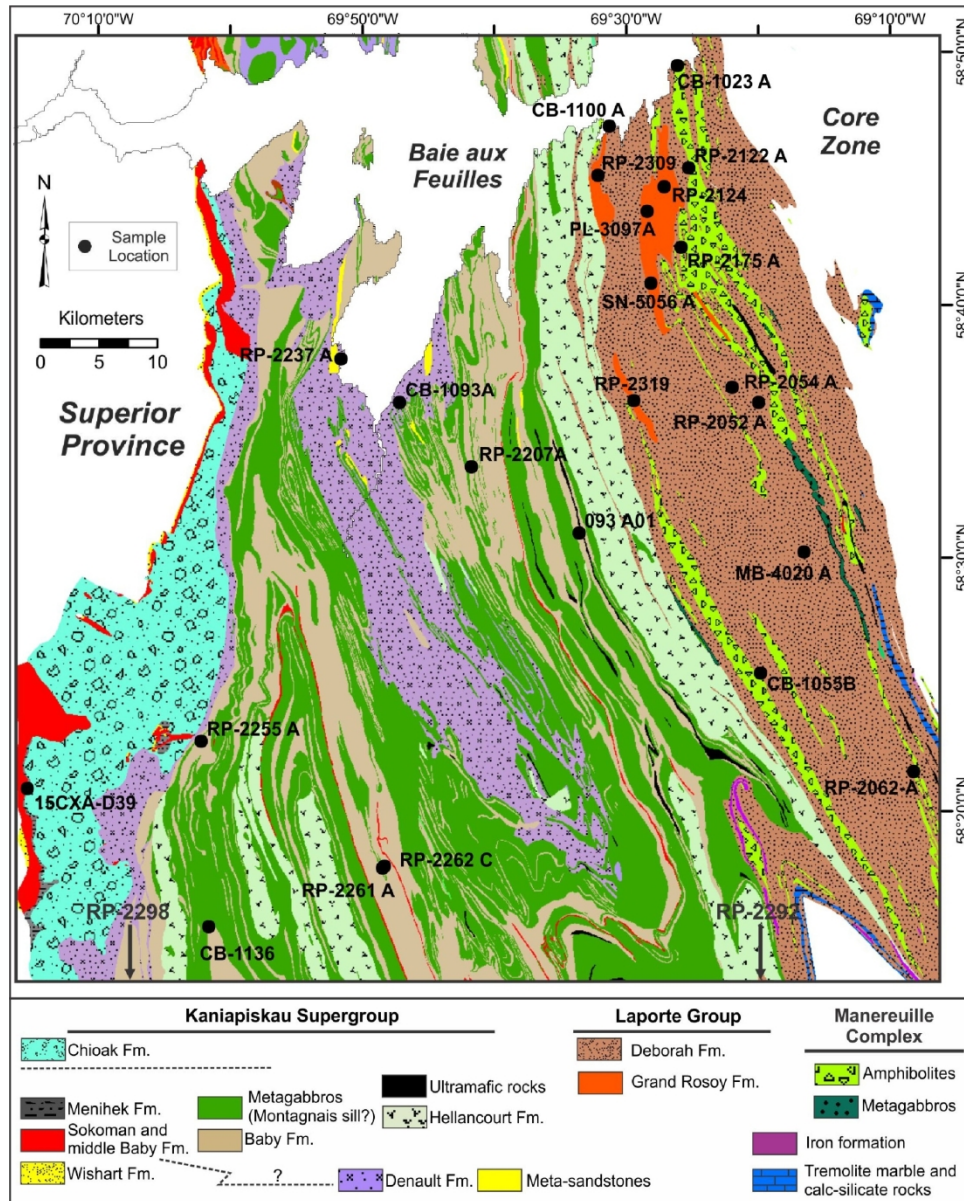


Fig. 2: Geological map of the Labrador Trough (north) showing parts of the Kaniapiskau Supergroup and Laporte Group, and the locations of dated samples (modified from <http://siggeom.mines.gouv.qc.ca>).

190x236mm (300 x 300 DPI)

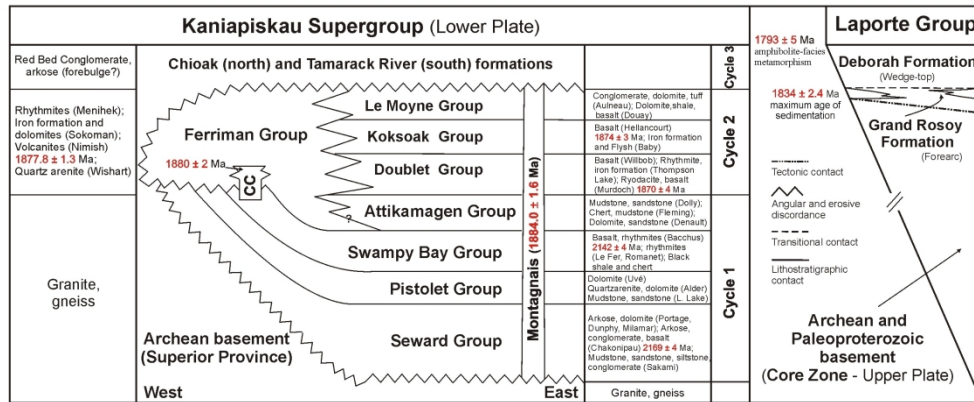


Fig. 3: Schematic stratigraphy of the Kaniapiskau Supergroup (modified from Clark and Wares, 2005). CC= Castignone Lake Carbonatite Complex.

236x98mm (300 x 300 DPI)

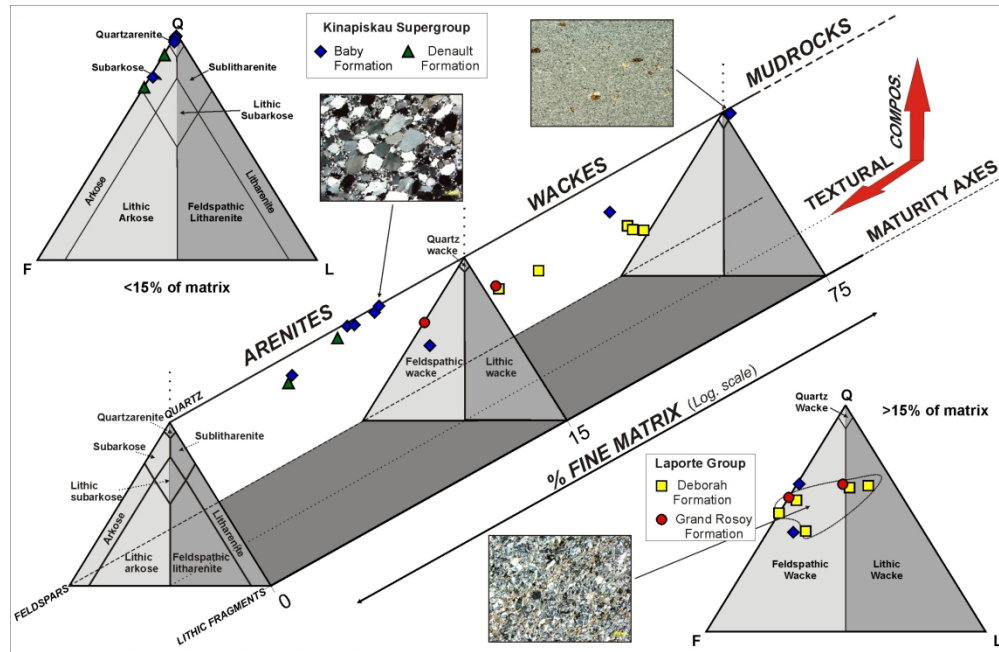


Fig. 4: Labrador Trough samples plotted on a QFL ternary diagram: Q=quartz, F=feldspar, L=lithic fragments. Fields after Dott (1964), McBride (1963) and Pettijohn (1975).

237x153mm (300 x 300 DPI)

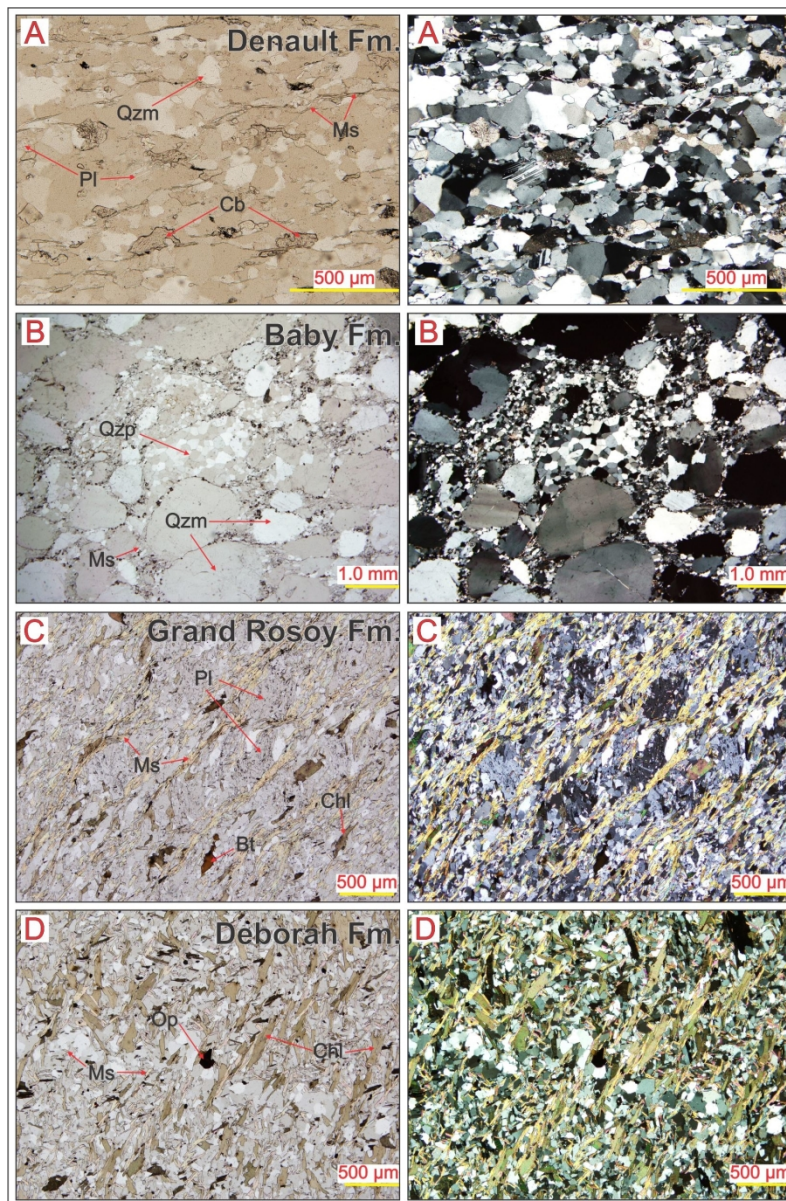


Fig. 5: Photomicrographs of metasedimentary rocks of the Kaniapiskau Supergroup and Laporte Group (left, parallel polarizers; right, crossed polarizers). A- subarkose from the Denault Formation; B- quartz arenite from the Baby Formation; C- feldspathic wacke from the Grand Rosoy Formation; D- quartz wacke from the Deborah Formation. Abbreviations: Qzp%= polycrystalline quartz; Qzm%= monocrystalline quartz; Qt%= total quartz; L%= lithic fragments; Ft%= total feldspars; Kfs= K-feldspar; Pl= plagioclase; Cb= carbonate; Op. min.= opaque minerals; Acc= Accessory.

139x210mm (300 x 300 DPI)

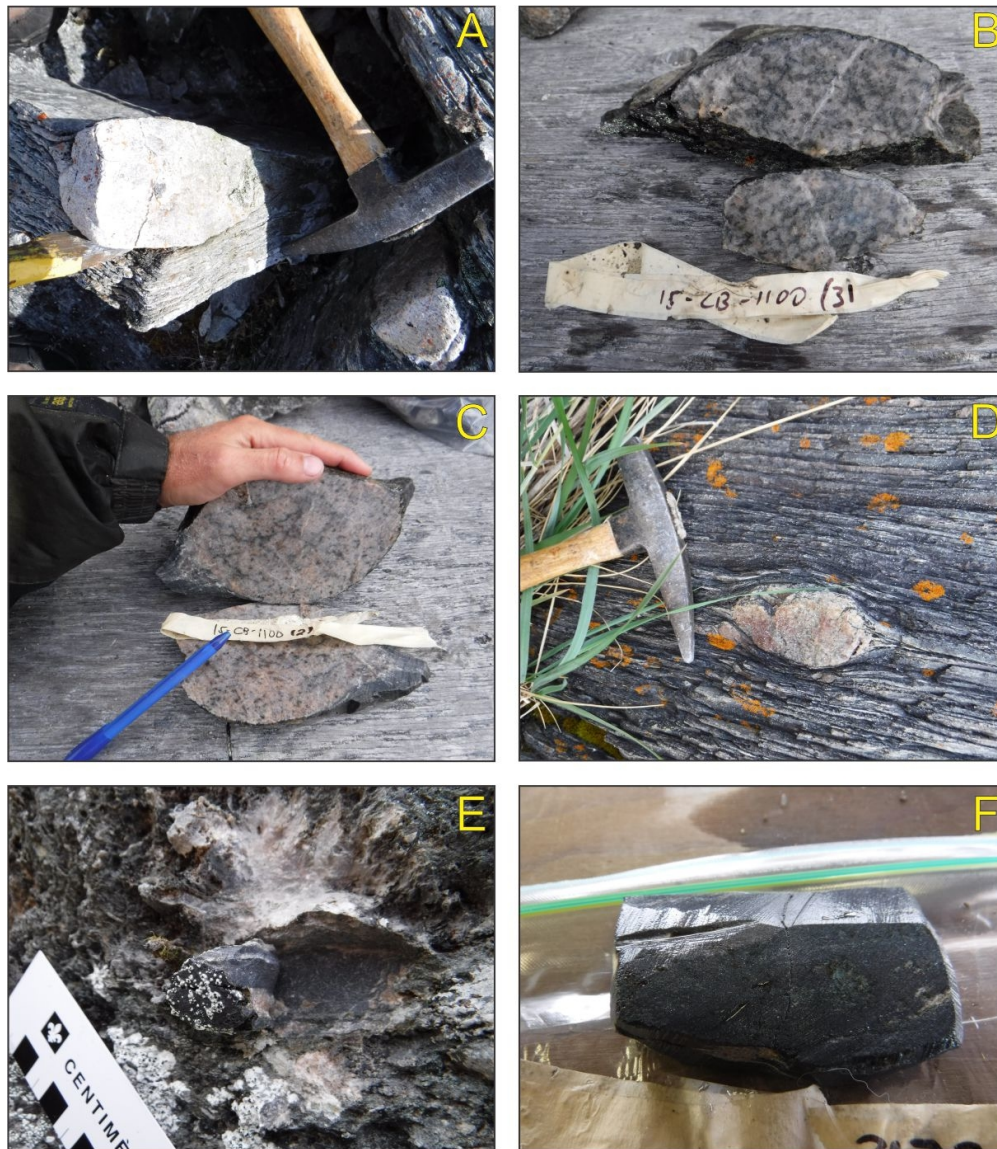


Fig. 6: Main clast variety of psephitic rocks from the Grand Rosoy Formation. A- quartz-rich leucocratic granodiorite; B- mesocratic monzogranite; C- leucocratic monzogranite; D- quartz-rich leucocratic alkali-feldspar granite; E and F- hematite-bearing iron formation.

102x117mm (300 x 300 DPI)

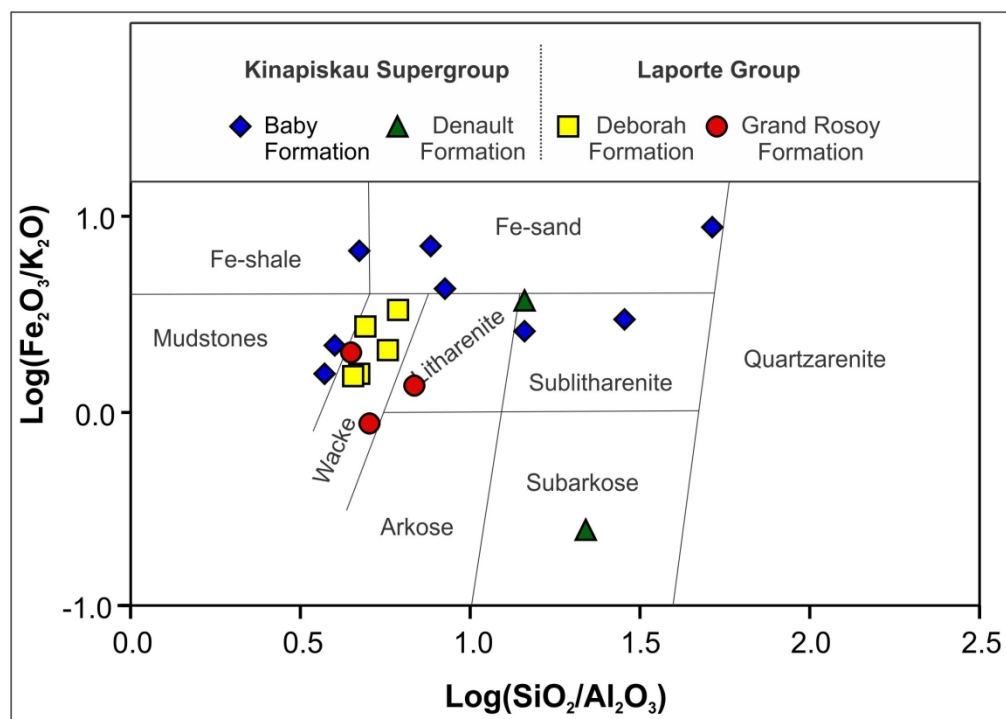


Fig. 7: Chemical classification diagram [$\log(\text{SiO}_2/\text{Al}_2\text{O}_3)$ versus $\log(\text{Fe}_2\text{O}_3/\text{K}_2\text{O})$] (Herron, 1988) for samples from the Kaniapiskau Supergroup and Laporte Group.

187x134mm (300 x 300 DPI)

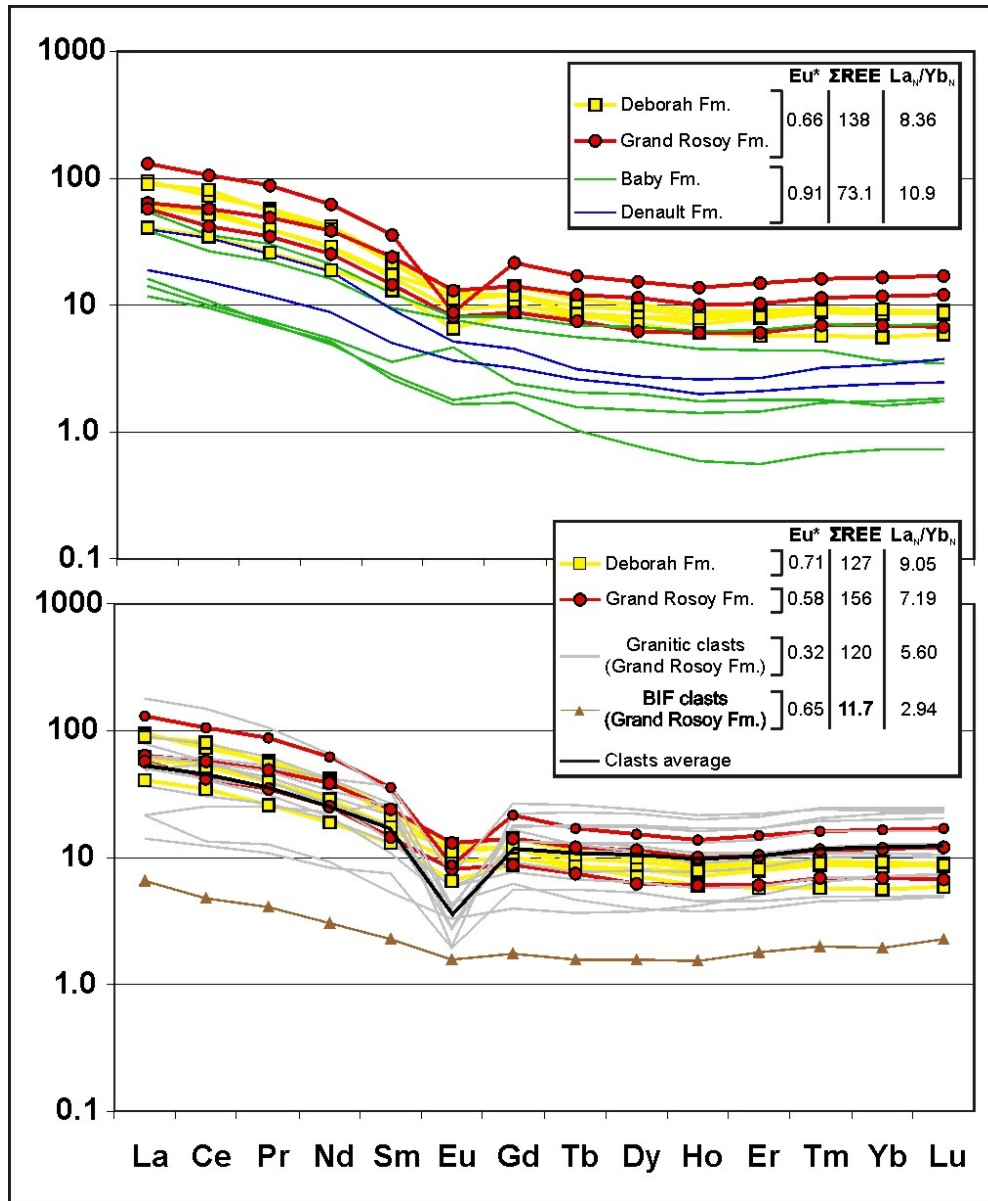


Fig. 8: Chondrite-normalized (Taylor and McLennan, 1985) rare-earth element patterns for metasedimentary rocks of the Labrador Trough.

86x103mm (300 x 300 DPI)

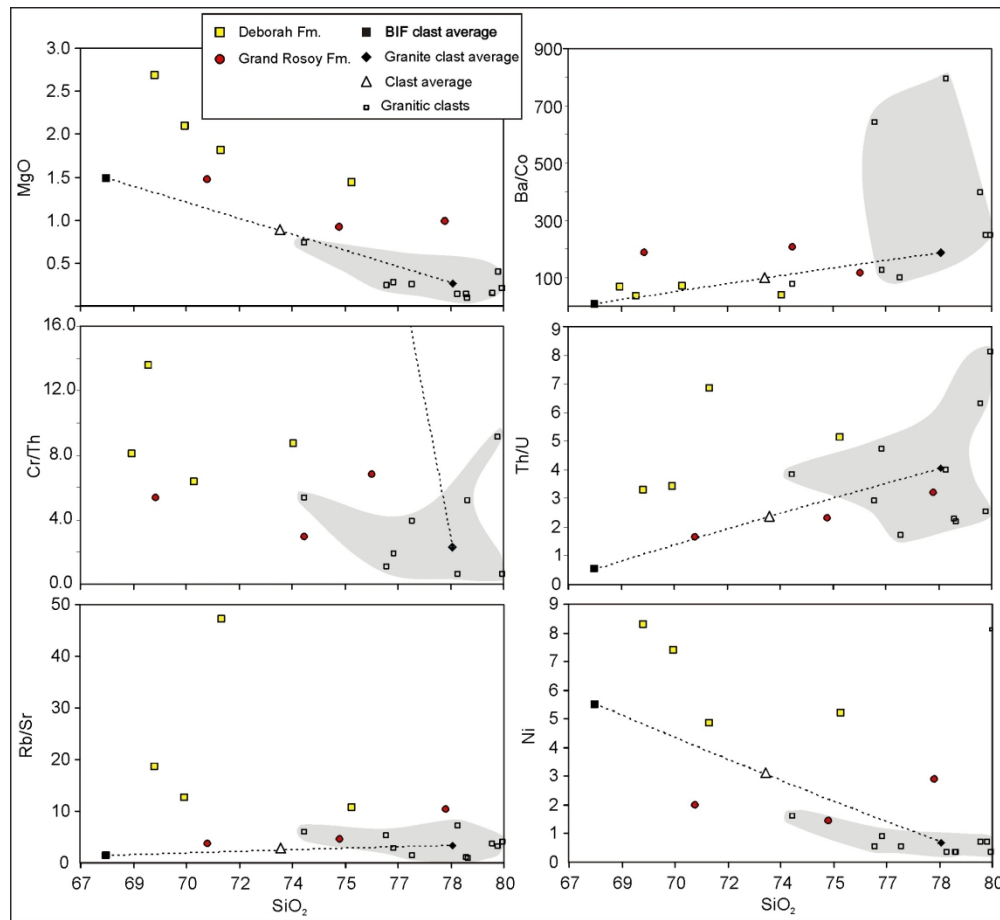


Fig. 9: Trace element variation diagrams versus SiO_2 in metasedimentary rocks of the Laporte Group. Grey shaded areas represent the range of granitic clast compositions.

182x166mm (300 x 300 DPI)

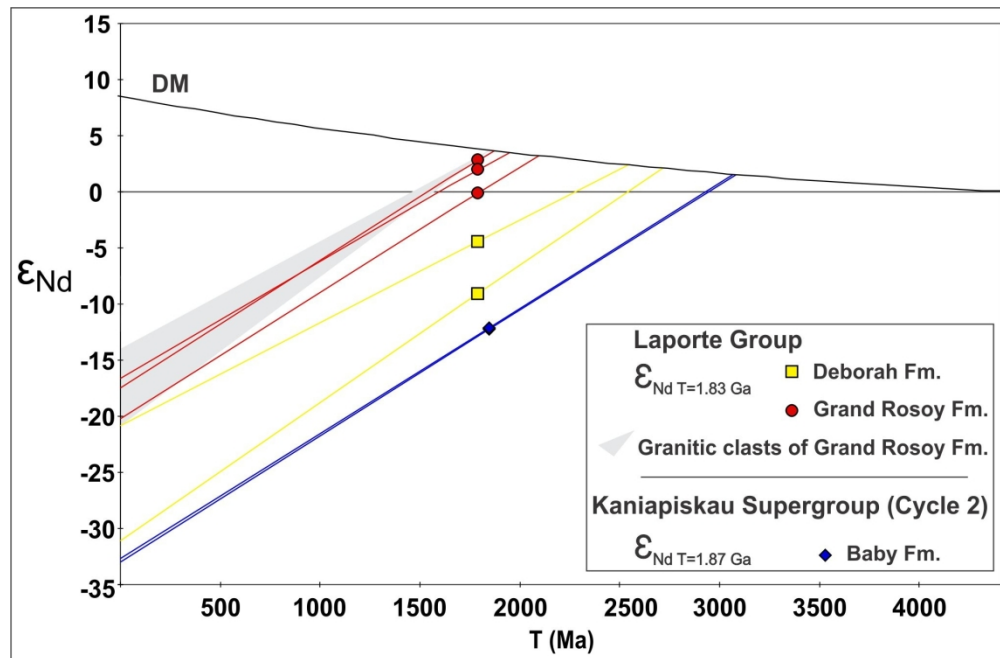


Fig. 10: ϵ_{Nd} versus TDM (Ga) diagram for metamudrocks and metawackes from the Kaniapiskau Supergroup and Laporte Group. DM = depleted mantle curve from De Paolo (1988).

173x113mm (300 x 300 DPI)

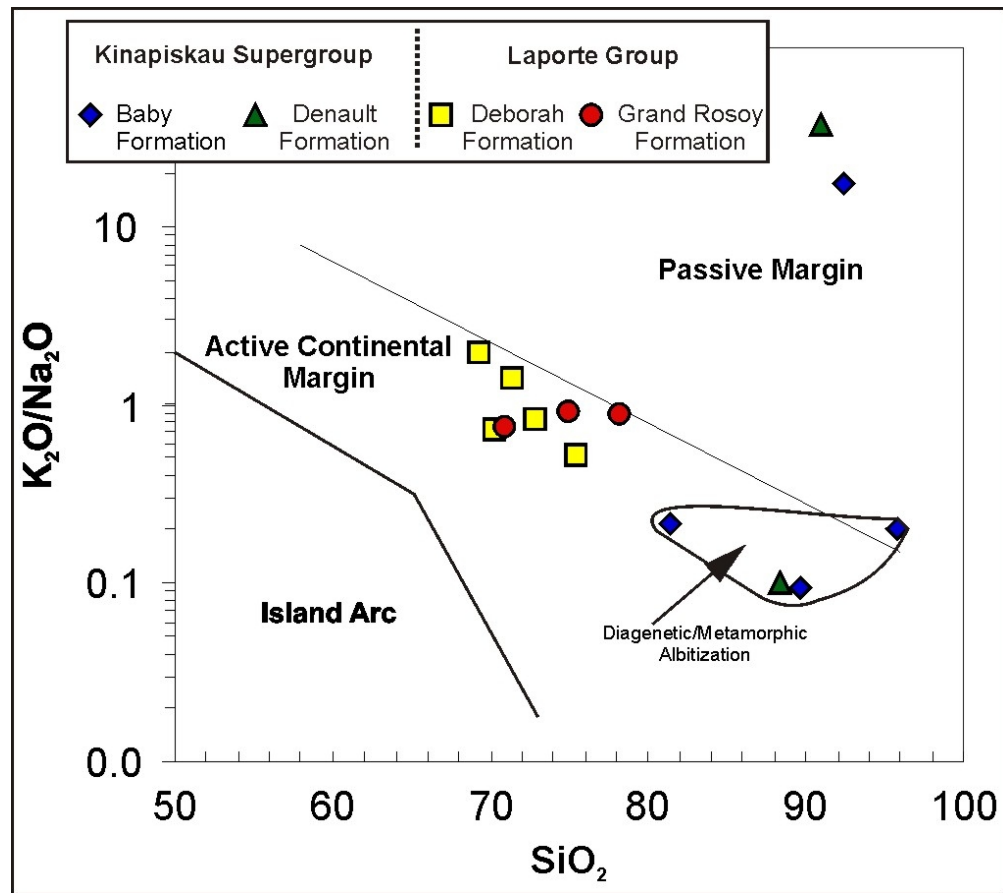


Fig. 11: Labrador Trough samples plotted on a K_2O/Na_2O vs. SiO_2 diagram (Roser and Korsch, 1986).

86x76mm (300 x 300 DPI)

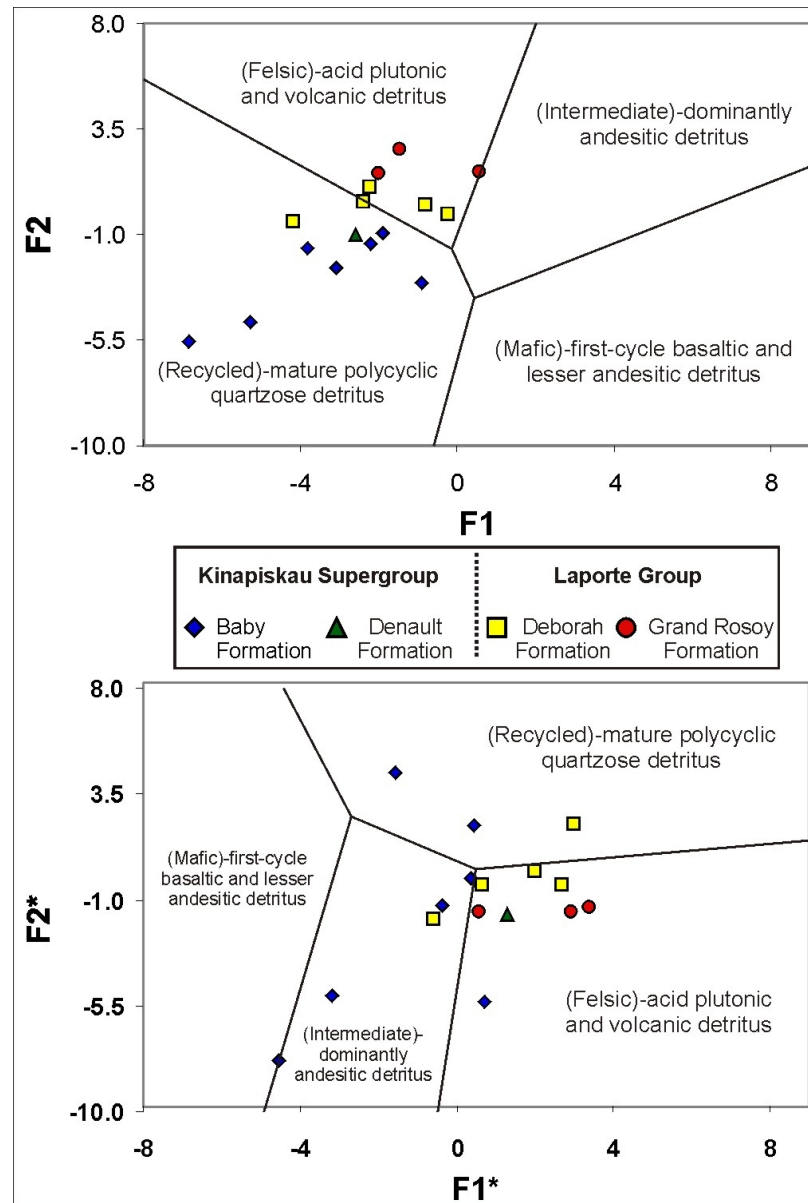


Fig. 12: Provenance signatures using discriminant function analysis from Roser and Korsch (1988) applied to rocks from the Kaniapiskau Supergroup and Laporte Group. The discriminant functions are: $F1 = (-1,773 \cdot TiO_2) + (0,607 \cdot Al_2O_3) + (0,76 \cdot Fe_2O_3) - (1,5 \cdot MgO) + (0,616 \cdot CaO) + (0,509 \cdot Na_2O) - (1,224 \cdot K_2O) - 9,09$; $F2 = (0,445 \cdot TiO_2) + (0,07 \cdot Al_2O_3) - (0,25 \cdot Fe_2O_3) - (1,142 \cdot MgO) + (0,438 \cdot CaO) + (1,475 \cdot Na_2O) + (1,426 \cdot K_2O) - 6,861$; $F1^* = (((30,638 \cdot TiO_2) / Al_2O_3) - (12,541 \cdot Fe_2O_3) / Al_2O_3) + ((7,329 \cdot MgO) / Al_2O_3) + ((12,031 \cdot Na_2O) / Al_2O_3) + ((35,402 \cdot K_2O) / Al_2O_3) - 6,382$; $F2^* = (((56,5 \cdot TiO_2) / Al_2O_3) - ((10,879 \cdot Fe_2O_3) / Al_2O_3) + ((30,875 \cdot MgO) / Al_2O_3) - ((5,404 \cdot Na_2O) / Al_2O_3) + ((11,112 \cdot K_2O) / Al_2O_3) - 3,89$.

86x127mm (300 x 300 DPI)

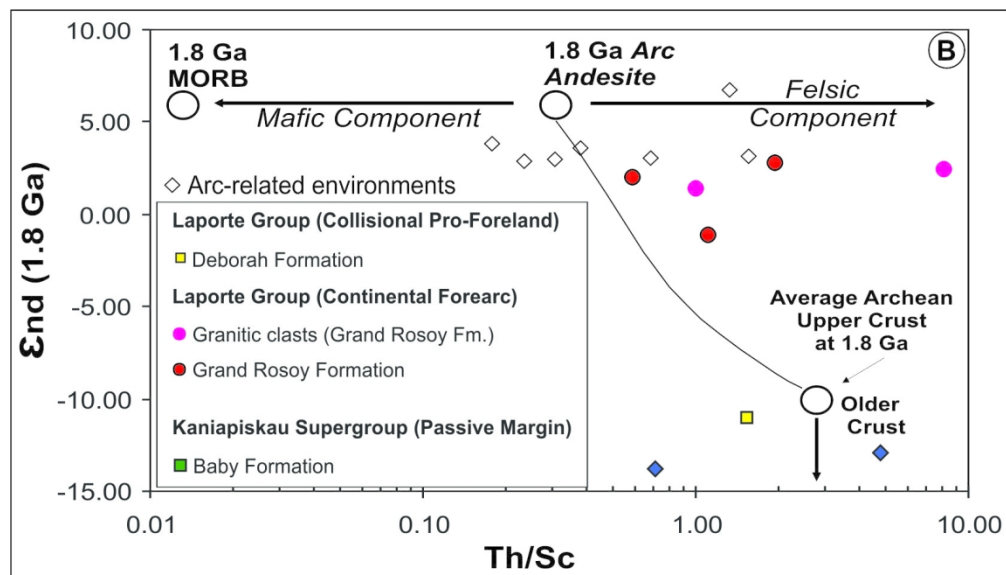


Fig. 13: Plot of ϵ_{Nd} versus Th/Sc ratio (McLennan et al., 1990) for metamudrocks and metawackes of the Kaniapiskau Supergroup and Laporte Group.

141x81mm (300 x 300 DPI)

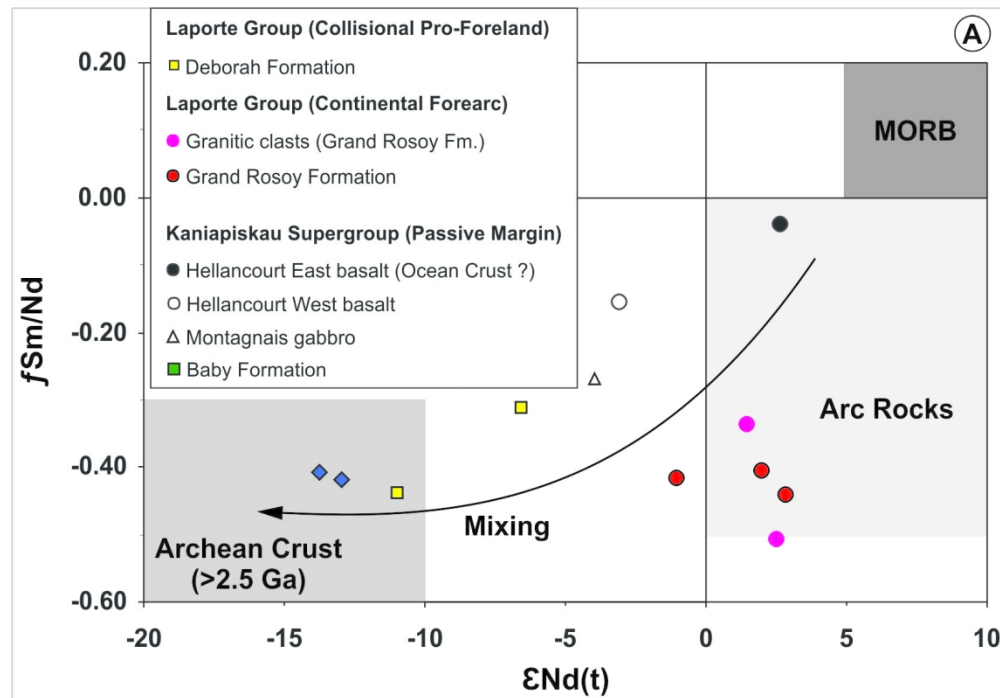


Fig. 14: Plot of fSm/Nd versus ϵNd (McLennan and Hemming, 1991) for metamudrocks, metawackes and metavolcanic rocks of the Kaniapiskau Supergroup and Laporte Group.

142x99mm (300 x 300 DPI)

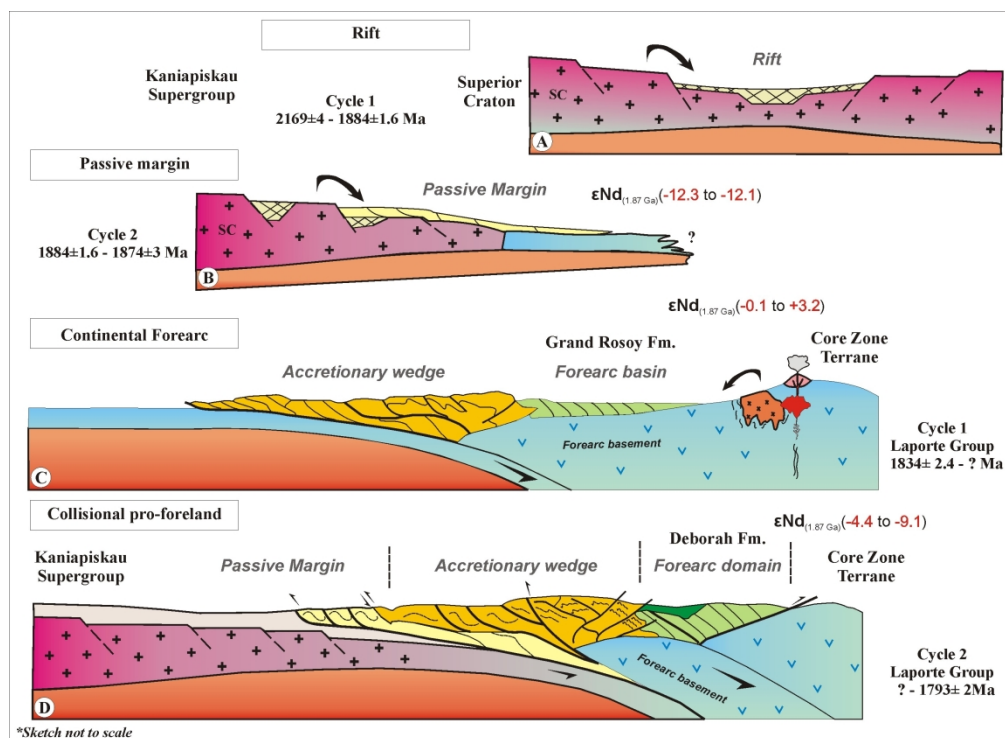


Fig. 15: Preferred tectonic model for the evolution of the New Quebec Orogen.

247x181mm (300 x 300 DPI)

	Samples	Qz-mon	Qz-poli	Kfs	Pl	lithic	accessory	fine-grain	Ms	Cb	Op	total	Matrix%	Qzp%	Qzm%	Qzt%	L%	Ft%	Kfs%	Pl%
Kaniapiskau Supergroup	RP-2231 A3 (Baby Fm.) *1	396	-	-	-	-	17	-	63	145	621	0	0	100	100	0	0	0	0	
	RP-2298 (Denault Fm.) *2	31	333	103	11	-	20	19	38	1	556	3	70	6	76	0	24	22	2	
	093-A01 (Baby Fm.) *2	233	232	45	38	5	10	24	13	-	600	4	42	42	84	0,9	15	8	7	
	RP-2237-A (Denault Fm.) *1	91	312	12	29	1	18	27	69	-	559	5	70	20	91	0,2	9	3	7	
	RP-2262-C (Baby Fm.) *1	282	175	-	14	-	7	41	35	1	555	7	37	60	97	0	3	0	3	
	RP-2255 (Baby Fm.) *1	109	321	-	2	-	5	55	31	16	539	10	74	25	100	0	0,5	0	0,5	
	RP-2292-B (Baby Fm.) *2	54	203	18	20	98	7	56	53	10	519	11	52	14	65	25	10	5	5	
	RP-2261 A1 (Baby Fm.) *3	181	226	13	43	-	4	113	37	-	617	18	49	39	88	0	12	3	9	
	RP-2292-A (Baby Fm.) *3	75	161	9	5	-	7	212	55	7	531	40	64	30	94	0	6	4	2	
	CB-1093-A (Baby Fm.) *4	147	-	-	-	-	42	555	-	-	744	75	0	100	100	0	0	0	0	
RP-2207-A (Baby Fm.) *4	146	-	-	-	-	9	460	-	-	615	75	0	100	100	0	0	0	0		
Laporte Group	Samples	Qz	Kfs	Pl	lithic	accessory	phyllosilicate	Cb	Op	total	Matrix%	-	-	Qt%	L%	F%	Kfs%	Pl%		
	RP-2309-B (Grand Rosoy Fm.)	405	81	2	-	33	104	-	-	625	17	-	-	89	0	11	11	0		
	RP-2052-A (Deborah Fm.)	343	43	-	-	43	123	-	-	552	22	-	-	99	0	1	1	0		
	RP-2319-A (Grand Rosoy Fm.)	355	59	3	-	2	135	7	-	561	24	-	-	85	0	15	14	0,7		
	MB-4020-A (Deborah Fm.)	389	96	-	-	17	168	-	-	670	25	-	-	100	0	0	0	0		
	CB-1023-A (Deborah Fm.)	363	4	-	-	12	200	3	-	582	34	-	-	80	0	20	20	0		
	PL-3247-A (Deborah Fm.)	344	4	-	-	8	182	-	-	538	34	-	-	99	0	1	1	0		
	RP-2054-A (Deborah Fm.)	256	-	-	-	18	275	-	-	549	50	-	-	83	0	17	17	0,4		

	sample name	age	Nd (ppm)	Sm (ppm)	Sm/Nd	143/144Nd	error (2 σ)	ϵ Nd(0)	ϵ Nd(t)	TDM	Th/Sc	fSm/Nd	ϵ Nd(TDM)
Laporte Group	Grand Rosoy Fm (clast-metaconglomerate)	1.82	47.2	7.45	0.0953	0.511572	0.000010	-20.8	2.9	2.0	8.08	-0.52	5.4
	Grand Rosoy Fm (clast-metaconglomerate)	1.82	14.0	2.85	0.1234	0.511922	0.000010	-14.0	3.2	2.1	1.00	-0.37	5.4
	Grand Rosoy Fm (meta-feldspathic wacke)	1.82	25.7	4.98	0.1170	0.511785	0.000079	-16.6	2.0	2.1	0.58	-0.41	5.2
	Grand Rosoy Fm (meta-feldspathic wacke)	1.82	45.1	8.21	0.1100	0.511744	0.000093	-17.4	2.8	2.1	1.94	-0.44	5.4
	Grand Rosoy Fm (meta-feldspathic wacke)	1.82	17.6	3.23	0.1109	0.511605	0.000011	-20.1	-0.1	2.3	1.11	-0.44	4.8
	Deborah Fm (meta-wacke)	1.82	13.5	2.83	0.1262	0.511568	0.000005	-20.9	-4.4	2.7	0.93	-0.36	3.8
Piskau Super	Deborah Fm (meta-wacke)	1.82	27.3	4.65	0.1027	0.511045	0.000014	-31.1	-9.1	2.9	1.53	-0.48	3.4
	Hellancourt (metabasalt) W part	1.87	18.0	4.16	0.1401	0.511823	0.000007	-15.9	-2.3	2.7	-	-0.29	3.9
	Hellancourt (meta-pillow basalt) E part	1.87	8.79	2.82	0.1940	0.512774	0.000019	2.7	3.3	-	-	-0.01	3.7
	Montagnais (metagabbro)	1.89	12.3	3.30	0.1614	0.512101	0.000048	-10.5	-1.9	-	-	-0.18	3.2
	Baby Fm (meta-mudrock)	1.87	15.1	2.77	0.1109	0.510961	0.000114	-32.7	-12.1	3.2	4.74	-0.44	2.6
	Baby Fm (meta-subarkose)	1.87	11.5	2.10	0.1107	0.510949	0.000014	-32.9	-12.3	3.2	0.71	-0.44	2.6